# A QUALITATIVE AND QUANTITATIVE STUDY OF THE LUNG OF AN OSTRICH, *STRUTHIO CAMELUS*

JOHN N. MAINA* AND CHRISTOPHER NATHANIEL

*Department of Anatomical Sciences, The University of the Witwatersrand, 7 York Road, Parktown, Johannesburg 2193, South Africa*

*e-mail: 055john@chiron.wits.ac.za

## Summary

The ostrich lung, with its lack of interparabronchial septa, the presence of very shallow atria and exceptional morphometric refinement, structurally resembles those of small, energetic flying birds, whereas it also displays features characteristic of the flightless ratites in which the neopulmo is relatively poorly developed and a segmentum accelerans may be generally lacking. The large size of the bronchial system of the ostrich may help explain the unique shifts in the airflow pathways that must occur from resting to panting breathing, explaining its insensitivity to acid–base imbalance of the blood during sustained panting under thermal stress. The mass-specific volume of the lung is $39.1\,cm^3\,kg^{-1}$ and the volume density of the exchange tissue is remarkably high (78.31 %). The blood–gas (tissue) barrier is relatively thick ($0.56\,\mu m$) but the plasma layer is very thin ($0.14\,\mu m$). In this flightless ratite bird, the mass-specific surface area of the tissue barrier ($30.1\,cm^2\,g^{-1}$), the mass-specific anatomical diffusing capacity of the tissue barrier for oxygen ($0.0022\,ml\,O_2\,s^{-1}\,Pa^{-1}\,kg^{-1}$), the mass-specific volume of pulmonary capillary blood ($6.25\,cm^3\,kg^{-1}$) and the mass-specific total anatomical diffusing capacity for oxygen ($0.00073\,ml\,O_2\,s^{-1}\,Pa^{-1}\,kg^{-1}$) are equivalent to or exceed those of much smaller highly aerobic volant birds. The distinctive morphological and morphometric features that seem to occur in the ostrich lung may explain how it achieves and maintains high aerobic capacities and endures long thermal panting without experiencing respiratory alkalosis.

Key words: ostrich, *Struthio camelus*, lung, ratite, birds, respiration, size, morphology, morphometry.

## Introduction

Originally comprising seven species of which only one now exists, the family Struthionidae evolved in the Lower Pliocene (approximately 7 million years ago), possibly around the Palearctic region (e.g. Fisher and Peterson, 1988; Pough et al., 1989). The earliest fossil materials have been found in Egypt, Greece, southern Russia, Iran, northern India and Mongolia. Exterminated from the Near-East and the Arabian Peninsula within the chronicled past, the geographical distribution of the ostrich (*Struthio camelus*) initially extended deep into the major deserts of Africa, especially the Sahara. At present, the bird is ecologically restricted to the semi-arid open savanna regions of the continent. Although not the heaviest bird by far that has ever lived (the elephant bird of Madagascar, *Aepyornis*, which became extinct about 350 years ago weighed nearly half a ton), standing approximately at 3 m and weighing as much as 160 kg at maturity (e.g. Fisher and Peterson, 1988), the ostrich is the largest extant bird. Compared with the tiny bee-hummingbird (*Calypte helenae*) of Cuba that measures only 5 cm from the beak-tip to tail-tip, has a wing span of only 10 cm and weighs only approximately 1.6 g, the ostrich is $10^5$ times heavier. Body mass is perhaps the most important variable that sets the physiologies of animals (e.g. Kleiber,

1947; Kleiber, 1961; Schmidt-Nielsen and Larimer, 1958; Leighton et al., 1966; Lasiewski and Dawson, 1967; Stahl, 1967; Lasiewski and Calder, 1971; Heusner, 1982; Heusner, 1983; Grubb, 1983; Peters, 1983; Schmidt-Nielsen, 1984; Else and Hubert, 1985; Suarez, 1996; Suarez, 1998; West et al., 1999; Jeong et al., 2000).

Among birds, the colossal body size, the relinquishment of volancy and survival in an exacting habitat should have imposed certain constraints and prescribed particular physiological and morphological novelties on the biology of the ostrich. Compared with the smaller volant birds that can utilize adiabatic cooling and convective heat loss at altitude, the ostrich has to tolerate extreme thermal stresses on the ground. This is exacerbated by the fact that it is too large to seek cover and protection easily in more hospitable microclimates that may chance in its ecosystem. The intense selective pressure that the ostrich has endured in the past is clearly demonstrated by the now very restricted distribution of a once very extensive natural geographical distribution. Animals that live in extreme environments (e.g. Schmidt-Nielsen, 1964; Dawson and Schmidt-Nielsen, 1964; King and Farner, 1964) and those that face intense selective pressures must inescapably evolve certain

adaptations or face extinction. Such features have been reported in the ostrich (e.g. Louw et al., 1969).

The physiology of the ratites, a taxon phylogenetically considered to fall among the most primitive of the extant birds (e.g. Storer, 1971a; Storer, 1971b), differs from that of other birds in certain fundamental ways. While other birds have a body temperature ranging from 40–42 °C (e.g. Irving and Krog, 1954; McNab, 1966), the large flightless birds generally have a lower body temperature that ranges from 38.1–39.7 °C (King and Farner, 1961; Bligh and Hartley, 1965; Crawford and Schmidt-Nielsen, 1967; Crawford and Lasiewski, 1968; Louw et al., 1969; Calder and Dawson, 1978; Jones et al., 1983). Of the seven species of birds studied by Lutz et al. (Lutz et al., 1974), the rhea *Rhea americana* had the highest oxygen affinity of blood ($P_{50}$=2.8 kPa). While Calder and Schmidt-Nielsen (Calder and Schmidt-Nielsen, 1966; Calder and Schmidt-Nielsen, 1968) demonstrated that many species of panting birds show extreme hyperventilatory hypocapnia and alkalosis after several hours of exposure to thermal stress, the ostrich and the emu, *Dromiceius novaehollandiae*, maintain resting values of arterial $P_{CO_2}$ ($Pa_{CO_2}$) and pH while panting continuously for as long a 6 h under high (56 °C) ambient temperature (Schmidt-Nielsen et al., 1969; Jones, 1982a; Jones et al., 1983). Studies that have alluded to the existence of a similar acid–base stabilizing peculiarity with thermal panting in nonratite birds (e.g. Calder and Schmidt-Nielsen, 1966; Calder and Schmidt-Nielsen, 1968; Bouverot et al., 1974; Marder et al., 1974; Marder and Arad, 1975; Ramirez and Bernstein, 1976; Krauzs et al., 1977) are somewhat equivocal owing to certain important departures in the experimental procedures applied compared with those used on the ostrich (Schmidt-Nielsen et al., 1969; Jones, 1982a) and the emu (Jones et al., 1983).

Although the anatomy of the air sacs has been studied (Macalister, 1864; Roché, 1888; Schulze, 1908; Bezuidenhout, 1981; Bezuidenhout et al., 1999), morphological and morphometric studies on the ostrich lung, which should greatly help explain the exceptional respiratory physiology of the bird, are lacking. The goal of this study was to outline, both qualitatively and quantitatively, the structure of the ostrich lung to attempt to answer the following fundamental question: how does the design of the ostrich lung explain the unique physiological processes by which the bird attains a remarkable exercise capacity and toleration of the most severe heat loads of any bird by sustained panting while maintaining $Pa_{CO_2}$ at near resting values, i.e. without experiencing acid–base imbalance of the blood? It is hoped that the details given here may help to explain or may be used to resolve the unsettled questions on the physiology of the avian respiratory system and that of the ostrich in particular.

## Materials and methods
### Fixation of the lung

An ostrich *Struthio camelus* (L.) that weighed 40 kg and became recumbent after developing muscular weakness of the legs of unknown aetiology while undergoing physiological experiments in the field (regarding mechanisms of brain cooling under ambient thermal loading) came to us courtesy of the Department of Physiology, University of the Witwatersrand. The animal was due to be released back into the wild after the end of the experiments. It was brought to our animal holding unit for close observation and better veterinary care. After 2 days, it showed no significant improvement in its health. Although it was appreciated that from observations made on a single specimen far-reaching deductions, especially of a morphometric nature, could only be drawn cautiously, in view of the complete dearth of data on the lungs of the ostrich and particularly the rarity of such an interesting animal under a condition allowing controlled fixation of the lungs for microscopy, we decided to carry out a qualitative and quantitative investigation.

The ostrich was killed by intravenous injection with 15 ml of Euthanase (200 mg cm$^3$ sodium barbitone) into the brachial vein. A ventral midline incision was made along the neck and the larynx, and the trachea was exteriorized and cannulated. Stock solution (3 l) of Cumplucad anatomic solution (CAS) (International Zaragoza, Spain; osmolarity, 360 mosmol l$^{-1}$) was instilled down the trachea from a height of 30 cm above the highest point (the sternum) of the supine bird (CAS is a recently marketed organic peroxide- and alcohol-based fixative). The trachea was ligated below the cannula, and the fixative was left in the lungs. After 3 h, the sternum was removed to expose the lungs and some of the unavoidably damaged air sacs. The angle of bifurcation of the trachea into the extrapulmonary primary bronchi (EPPB) was determined while the lungs were still *in situ*, i.e. in their anatomical positions. Together with the attached trachea, the lungs were carefully dissected out from the deep costal insertions and immersed in fresh fixative. They were closely examined and found to be free of disease and physical damage. The lengths and diameters of the trachea, the EPPB, the intrapulmonary primary bronchi (IPPB), i.e. the mesobronchi, as well as the angles between the IPPB and the medioventral secondary bronchi (MVSB), were determined. The angles and diameters of the MVSB were measured after the lung had been isolated from the EPPB, dissected and a cast impression made using dental plastic (Pratley).

### Determination of the volume of the lung

The connective tissue and fat adherent to the lung were trimmed off. The large ostium opening into the caudal thoracic and abdominal air sacs and the opening to the EPPB (at the hilus) were plugged tightly with plastic paper (to avoid entry of water into the lung), and the volumes of the left and right lungs were individually determined by the water displacement method. A lung was slowly immersed into a container completely filled with water, the displaced water was collected in an outer container and the volume measured. Estimations were repeated, each time after mopping the lung dry, until three consistent values were obtained. The mean of such readings was taken to be the volume of the lung. The right lung was used for morphometric analysis and the left for morphological study.

Table 1. *Summary of the morphometric parameters directly determined on the lung of the ostrich,* Struthio camelus

| Magnification | Procedure | Variable | Symbol | Value | Units |
|---|---|---|---|---|---|
| ×18000 (TEM) | Intercept length measurement | Harmonic mean thickness: | | | μm |
| | | blood–gas barrier | $\tau$ht | 0.56 | |
| | | plasma layer | $\tau$hp | 0.14 | |
| | | Arithmetic mean of | | | |
| | | blood–gas barrier | $\tau$t | 0.69 | |
| **(A)** | | | | | |
| ×3200 (LM) | Point counting | Volume density: | $V_V$ | | |
| | | blood capillaries | $V_V$bc | 20.41 | % |
| | | | | (250) | $cm^3$ |
| | | air capillaries | $V_V$ac | 61.19 | % |
| | | | | (749) | $cm^3$ |
| | | blood–gas barrier | $V_V$bg | 12.69 | % |
| | | | | (155) | $cm^3$ |
| | | tissue not involved in gas exchange | $V_V$te | 5.71 (70) | % $cm^3$ |
| | Intersection counting | Surface density: | $S_V$ | | |
| | | erythrocytes | $S_V$er | 97.64 | $mm^2\,mm^{-3}$ |
| | | | | (120) | $m^2$ |
| | | capillary endothelium | $S_V$ce | 119.33 | $mm^2\,mm^{-3}$ |
| | | | | (146) | $m^2$ |
| | | air capillaries | $S_V$ac | 149 | $mm^2\,mm^{-3}$ |
| | | | | (183) | $m^2$ |
| | | blood-gas barrier | $S_V$bg | 98.32 | $mm^2\,mm^{-3}$ |
| | | | | (120) | $m^2$ |
| | | tissue not involved in gas exchange | $S_V$tg | 50.79 (63) | $mm^2\,mm^{-3}$ $m^2$ |
| **(B)** | | | | | |
| ×100 (LM) | Point counting | Volume density: | $V_V$ | | |
| | | exchange tissue | $V_V$et | 78.31 | % |
| | | | | (1224) | $cm^3$ |
| | | parabronchial lumen | $V_V$pl | 11.75 | % |
| | | | | (183) | $cm^3$ |
| | | smaller blood vessels <20 μm diameter | $V_V$sv | 9.94 (155) | % $cm^3$ |
| **(C)** | | | | | |
| ×1 (gross) | Point counting | Volume density: | $V_V$ | | |
| | | exchange tissue | $V_V$et | 89.92 | % |
| | | | | (1405) | $cm^3$ |
| | | large blood vessels (<0.5 mm diameter) | $V_V$lb | 4.38 (68) | % $cm^3$ |
| | | primary bronchus | $V_V$pb | 4.07 (64) | % $cm^3$ |
| | | secondary bronchi and parabronchi | $V_V$sp | 1.63 (25) | % $cm^3$ |

The hierarchical structure outlined can be used to reconstruct the variables and determine absolute values such as volumes and surface areas. The total volume of the lung was 1563 $cm^3$.

Reference volumes at different levels of analysis: A, exchange tissue; B, C, lung.

LM, light microscopy; TEM, transmission electron microscopy.

The numbers given in parentheses are the absolute values.

*Sampling and morphometric analyses of the lung*

Three dorsoventral cuts were made along the last three most prominent costal sulci of the right lung, giving four parts; the first sulcus was avoided because it was relatively more superficial, and a slice made along it would not pass through the primary bronchus owing to the caudomedial location of the hilus. The avian lung being reasonably homogeneous, especially at the parabronchial and parenchymal levels (e.g. Maina, 1988), the sulci were taken as predetermined (unbiased) sampling landmarks from which complete cross sections of the lung were taken craniocaudally (rather like stratified serial sections) for both light and transmission electron microscopic analyses.

Table 2. *Volume densities (%) of the main components of the lung of the ostrich compared with seven species of birds*

| | N | Exchange tissue $V_{\text{vet}}$ | Parabronchial lumen $V_{\text{vpl}}$ | Smaller blood vessels 20 μm/0.5 mm diameter $V_{\text{vsv}}$ | Primary bronchus $V_{\text{vpb}}$ |
|---|---|---|---|---|---|
| Ostrich *Struthio camelus* | 1 | 78.31 | 11.75 | 9.94 | 4.07 |
| Emu *Dromiceius novaehollandiae* | 1 | 17.76 | 49.11 | 28.57 | 4.56 |
| Penguin *Spheniscus humboldti* | 1 | 51.29 | 37.71 | 7.44 | 3.56 |
| Domestic fowl *Gallus gallus* var. *domesticus* | 3 | 46.35 | 30.56 | 13.65 | 9.34 |
| Goose *Anser anser* | 5 | 40.31 | 50.49 | 6.91 | 1.73 |
| Hummingbird *Colibri coruscans* | 3 | 46.4 | – | 13.6 | 11.4 |
| Herring gull *Larus argentatus* | 2 | 32.6 | 60.41 | 5.56 | 1.39 |
| House sparrow *Passer domesticus* | 5 | 55.68 | 36.91 | 6.45 | 0.96 |

Sources of data: ostrich, present study; emu, Maina and King, 1989; penguin, Maina and King, 1987; domestic fowl, Abdalla et al., 1982; goose, Maina and King, 1982; hummingbird, Dubach, 1981; herring gull, Maina, 1982, 1987; and house sparrow, Maina, 1984.

A quadratic lattice grid was laid on the cranial face of each slice, and the volume densities ($V_V$) of the exchange tissue ($V_{\text{vet}}$), the lumina of the secondary bronchi and parabronchi (tertiary bronchi) ($V_{\text{vsp}}$), the large blood vessels (<0.5 mm diameter) ($V_{\text{vlb}}$) and the primary bronchus ($V_{\text{vpb}}$) were determined: this constituted the first level (gross) of the four strata of the morphometric analyses (see Table 1). With the cranial face uppermost, the slices were laid out flat and cut into dorsal and ventral parts immediately dorsal to the IPPB. This gave rise to a total of eight half-slices that were lettered from A to H. Along their craniocaudal thicknesses, the half-slices were subsequently cut into halves: these are referred to as half-half-slices.

For light microscopic analysis, tissue samples were taken from the dorsal, middle, medial and lateral aspects of each caudal half-half-slice: 32 pieces, i.e. four pieces derived from each of the eight half-half-slices, were taken. For transmission electron microscopic sampling, a quadratic lattice grid with numbered squares was placed on each of the cranial half-half-slices. Random numbers were generated from a Casio Micronata Advanced Scientific Calculator (model 65-820: EC-4041), and six small pieces of lung tissue were taken from the squares representing the generated numbers. The samples were taken from the entire thickness of the slice: 48 pieces, i.e. six pieces from each of the eight cranial half-half slices, were taken and diced to a size of 1 mm³.

### Light microscopy

Tissue samples for light microscopy were processed by standard laboratory techniques and embedded in paraffin wax. Sections were cut at a thickness of 10 μm, stretched out on a hot water bath (40 °C), mounted on glass slides and stained with Haematoxylin and Eosin. Comparison of the dimensions of the mounted and stained sections with the size of the tissue block face was used to check for compression of the sections. From each tissue sample, the first technically adequate, i.e. non-compressed, well-stained section was used for morphometric analysis. The volume densities of the exchange tissue ($V_{\text{vet}}$), the lumina of the parabronchi ($V_{\text{vpl}}$), the blood vessels between 20 μm and 0.5 mm in diameter ($V_{\text{vsv}}$) were

determined by point-counting using an ocular Zeiss integrating graticule with an etched quadratic lattice grid at a magnification of ×100: the analysis was carried out field by field until the entire section had been covered: this constituted the second level of the morphometric analyses (see Table 1). To determine the adequacy of the sections analysed, a summation average graph was plotted, and the points counted were checked against a standard nomogram given by Weibel (Weibel, 1979, p. 114). Except for the primary bronchus, which constituted a relatively small fraction of the lung, the number of points counted for each of the structural components gave a standard error of less than 2 %.

### Transmission electron microscopy

Since the effectiveness and permanence of CAS in fixing tissues for transmission electron microscopy was uncertain, the sampled pieces were 'refixed' in 2.3 % glutaraldehyde buffered in sodium cacodylate (osmolarity 360 mosmol l⁻¹; pH 7.4 at 23 °C) for 6 h. Subsequently, for 3 h, the tissue samples were post-fixed in 1 % osmium tetroxide buffered in 1 mol l⁻¹ sodium cacodylate (pH 7.4 at 23 °C; total osmolarity 350 mosmol l⁻¹). This was followed by block staining with 0.5 % uranyl acetate buffered with 0.05 mol l⁻¹ sodium hydride maleate adjusted by sodium hydroxide (pH 4.8 at 23 °C; total osmolarity 100 mosmol l⁻¹). The tissues were dehydrated in a graded series of ethanol concentrations from 70 % to absolute and two changes in acetone, then infiltrated and embedded in epoxy resin (Epon 812).

Blocks were prepared from pieces derived from different areas of a half-half-slice, a block was picked at random, and semithin sections were cut and stained with Toluidene Blue. The sections were viewed on a Kontron Image Analyzer (Zeiss Instruments) at a magnification of ×3200 with a superimposed quadratic lattice grid: this constituted the third level of the hierarchical morphometric analyses (Table 1). The volume densities of the components of the exchange tissue, i.e. the air capillaries ($V_{\text{vac}}$), blood capillaries ($V_{\text{vbc}}$) and supporting tissue [i.e. the tissue involved in gas exchange (tissue of the blood–gas barrier, $V_{\text{vbg}}$), and the tissue not involved in gas

exchange, $V_V$te (i.e. where blood or air capillaries directly connect; see Fig. 10)] were determined by point-counting. The surface densities ($S_V$) of the air capillaries ($S_V$ac), blood–gas (tissue) barrier ($S_V$bg), capillary endothelium ($S_V$ce), erythrocytes ($S_V$er) and tissue not involved in gas exchange ($S_V$te) were determined by intersection-counting (Weibel, 1979). The absolute volumes and the surface areas were calculated from the volumes of the lung and that of the exchange tissue ($V$et), as appropriate. The surface area of the plasma layer was estimated as the mean of that of the capillary endothelium and the erythrocytes and the surface density of the blood–gas tissue barrier as the ratio of its surface area to $V$et.

Ultrathin sections were cut from the trimmed blocks on which the semithin sections were acquired and mounted on 200-wire-mesh carbon-coated copper grids, counterstained with 2.5 % lead citrate and examined on a Hitachi 800A transmission electron microscope at an accelerating voltage of 80 kV. From blocks prepared from each of the eight half-half-slices, 25 pictures were taken at a primary magnification of ×6000 from predetermined corners of the grid squares to avoid bias: 200 electron micrographs were analysed. The negatives were printed at an enlargement factor of ×3, giving a secondary magnification of ×18 000: that constituted the fourth level of the stratified morphometric analyses (Table 2). A quadratic (square) lattice test grid was superimposed and printed directly onto the electron micrographs. Intercepts were measured for determination of the harmonic mean thicknesses of the blood–gas (tissue) barrier ($τ$ht) and the plasma layer ($τ$hp) (e.g. Weibel and Knight, 1964; Weibel, 1970/71). The harmonic mean values were multiplied by a factor of two-thirds to correct for an overestimate due to random orientation and obliqueness of sectioning. The relevant morphometric data were modelled to estimate the diffusing capacities (conductances) of the components of the air–haemoglobin pathway, namely the tissue barrier ($D$t$_{O_2}$), the plasma layer ($D$p$_{O_2}$) and the erythrocytes ($D$e$_{O_2}$) (Weibel, 1970/71). Except for $D$t$_{O_2}$, the maximum and minimum values were calculated from the available physical constants: from these values, the membrane ($D$m$_{O_2}$) and the total morphometric pulmonary diffusing capacity ($D$L$_{O_2}$) was calculated. The methods used here, as applied to the avian lung, are given in detail and critically discussed in Maina

et al. (Maina et al., 1989). Weibel (Weibel, 1990) and Weibel et al. (Weibel et al., 1993) discussed the limitations inherent in pulmonary morphometric analysis and modelling, particularly the uncertainties regarding the plasma layer.

### Scanning electron microscopy

Samples were taken from various parts of the left lung and prepared for scanning electron microscopy. To ensure satisfactory fixation, they were first placed in 2.3 % glutaraldehyde buffered in sodium cacodylate for 2 weeks. The pieces were subsequently dehydrated in five changes of absolute alcohol over a period of 2 weeks, critical-point-dried in liquid carbon dioxide, mounted on aluminium stubs and sputter-coated with gold–palladium complex before viewing on a JEOL (JSM 840) scanning electron microscope at an accelerating voltage of 15 kV.

### Computer-generated three-dimensional structural model

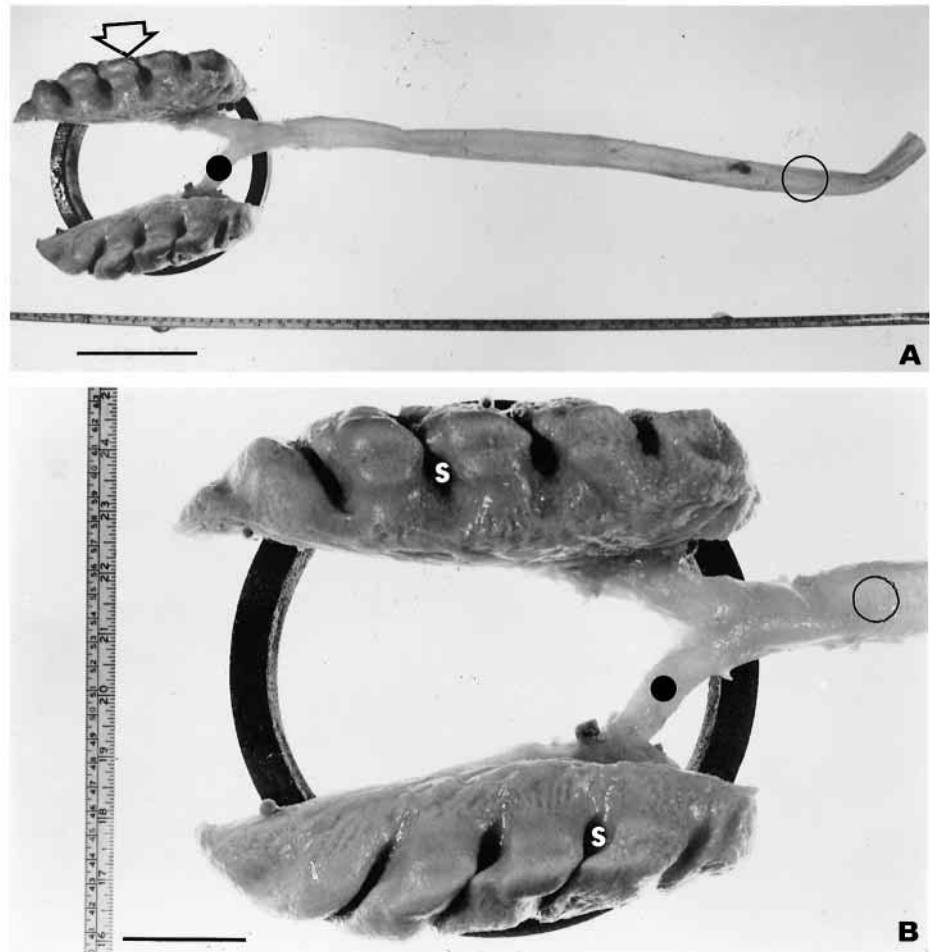On the basis of the actual dimensions and geometries of the



Fig. 1 (A). Dorsal view of the trachea (circled) and the lung of the ostrich *Struthio camelus*. The lungs are deeply entrenched into the ribs on the dorsolateral aspects (arrowhead). Filled circle, right extrapulmonary primary bronchus (EPPB). Note that the right EPPB is relatively longer, rather horizontal and relatively narrower compared with the left EPPB. Scale bar, 1 cm. (B) Close up of the dorsal aspect of the lung showing the deep costal sulci (s). Trachea, circled; filled circle, right extrapulmonary primary bronchus. Scale bar, 2 cm.

trachea, EPPP, IPPB and MVSB, a three-dimensional model of the conduits that are directly involved in inspiratory aerodynamic valving (IAV), a process through which the inspired air is shunted across the openings of the MVSB (e.g. Banzett et al., 1987; Butler et al., 1988; Wang et al., 1992) was drawn in CFX 5.4, a computational fluid dynamics (CFD) program. Compared with certain other birds (Maina and Africa, 2000), the ostrich lacks a segmentum accelerans (SA) at the terminal part of the EPPB. Conceivably, in the ostrich, the exceptionally large sizes and the particular geometry of the bronchial system in an exceptionally large bird may explain IAV: the airflow dynamics in the airways of the lung may differ significantly from those in the smaller birds. CFD is a computer-based tool for simulating the behaviour of systems involving fluid flow, heat transfer and other related physical processes. The technical and mathematical details entailed in the plotting, simulation of the airflow and interpretation of the results will be reported in a subsequent paper. Here, reconstructed three-dimensional views of the geometry and the relative sizes of the air-conduits involved in IAV (see Fig. 11) are given to help the reader sufficiently to conceptualize the morphological descriptions. Certain deviations from the actual geometry were inevitable because of software limitations and the complexity of the airway system itself. Furthermore, the diameters and the lengths of all the airtubes are shown as fixed, implying a rigid structure. This may not be the case in life.

### Results

The ostrich investigated in this study weighed 40 kg. Deep costal impressions occurred on the dorsal and lateral aspects of the lung (Fig. 1). The volume of the left lung was 815 cm$^3$ while that of the right lung was smaller (748 cm$^3$). Certain measurements regarding the length, diameter and angles of the trachea, the EPPB, the IPPB and the MVSB are shown diagrammatically in Fig. 2. The total length of the trachea from the larynx to its bifurcation was 78 cm, and the diameter (2 cm) was fairly constant. The syringeal constriction was 0.3 cm wide. The EPPB (measured from the syrinx to the origin of the first MVSB) was longer on the right side (5 cm) than on the left (4 cm). The right EPPB was narrower, longer and more horizontal than the left one, which was relatively wider, shorter and more vertical (Fig. 1). The length of the IPPB on the right lung was 9.6 cm and that on the left 9.8 cm. The diameter of the IPPB decreased gradually from 2.5 cm at the hilus (cranial end) to 1 cm at the caudal (ostial) end. Three MVSB (Fig. 3, Fig. 4, Fig. 5) and five mediodorsal secondary bronchi (MDSB) (Fig. 4, Fig. 6) were observed. The MVSB gave rise to various smaller branches. The angles between the IPPB and the MVSB were 140 ° for the cranial, 65 ° for the middle and 45 ° for the caudal bronchus (Fig. 2, Fig. 4): the diameters of the MVSB were 1.7 cm, 1.3 cm and 1.2 cm, respectively. The MVSB and the MDSB were interconnected by the many parabronchi (Fig. 3, Fig. 6, Fig. 7, Fig. 8A) that constitute the paleopulmo: the neopulmo was located on the ventromedial aspect of the lung close to the caudal air sacs and was relatively
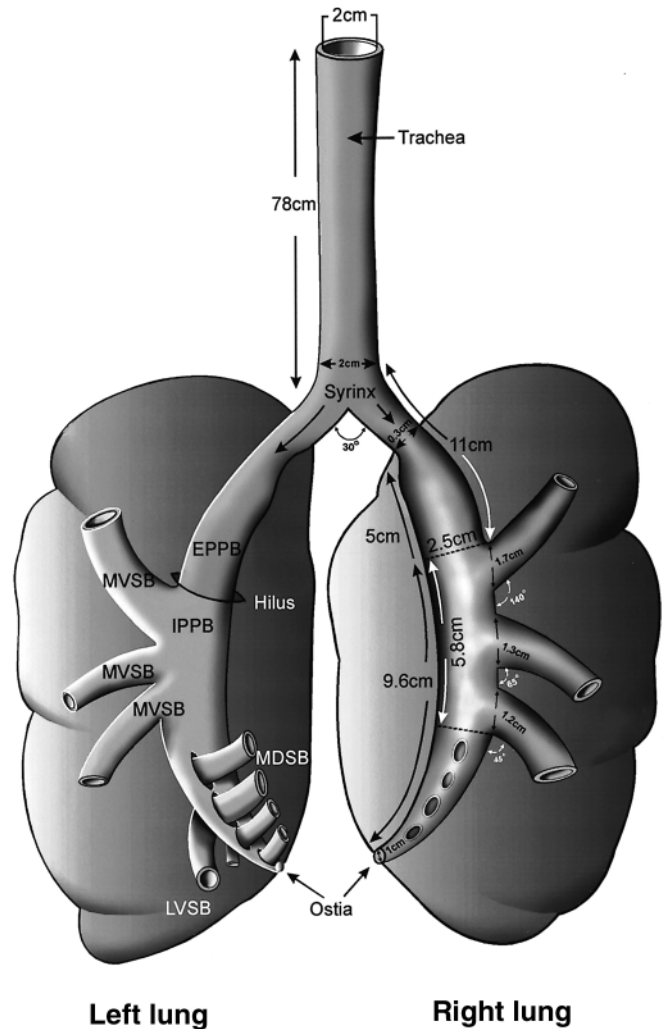


Fig. 2. A schematic illustration of the lung of the ostrich *Struthio camelus* showing various measurements of the air conduits. EPPB, extrapulmonary primary bronchus; IPPB, intrapulmonary primary bronchus; MVSB, medioventral secondary bronchi; MDSB, mediodorsal secondary bronchi; LVSB, lateral ventral secondary bronchus.

poorly developed (Fig. 4). This particularly exposed the MDSB on the lateral aspect of the lung (Fig. 6). The parabronchial lumina were surrounded by exchange tissue (Fig. 8B), the interparabronchial septa were conspicuously lacking, the atrial muscles were poorly developed and the atria were shallow (Fig. 8B, Fig. 9). The average diameter of the air capillaries was 20 µm (Fig. 10A) and the blood–gas (tissue) barrier was sporadically attenuated (Fig. 10B). The three-dimensional disposition of the EPPB, MVSB and the IPPB are shown in the computer-generated models (Fig. 11) based on actual measurements (Fig. 2).

The stratification of the experimental design and the relative and absolute morphometric values are given in Table 1. Comparisons of the ostrich data with those of seven other species selected on the basis of body size, phylogenetic levels of development within the avian taxon (e.g. Storer, 1971b) and

lifestyle are given in Table 2, Table 3, Table 4 and Table 5. $Dt_{O_2}$ was $0.0881\,ml\,O_2\,s^{-1}\,Pa^{-1}$; $Dp_{O_2}$ ranged from $0.3794$ to $0.5123\,ml\,O_2\,s^{-1}\,Pa^{-1}$; $De_{O_2}$ ranged from $0.0282$ to $0.0782\,ml\,O_2\,s^{-1}\,Pa^{-1}$; $Dm_{O_2}$ ranged from $0.0715$ to $0.0752\,ml\,O_2\,s^{-1}\,Pa^{-1}$ and $DL_{O_2}$ ranged from $0.0202$ to $0.0383\,ml\,O_2\,s^{-1}\,Pa^{-1}$.

## Discussion

In the remarkably speciose avian taxon that consists of approximately 9000 species (e.g. Morony et al., 1975; Gruson, 1976), the ostrich is of special interest, First, because of its size, it is of great importance for understanding the underlying constraints in the allometric scaling of morphological variables and physiological processes in birds. Second, in avian phylogeny, the ratites [a diffuse group of birds that show remarkable parallel evolution in widely separated parts of the world, e.g. ostrich (Africa), rhea (South America), emu and cassowary (Australia), kiwis (New Zealand) and perhaps tinamous (Central and South America)], are a unique group of large flightless birds of the Southern Hemisphere that share interesting common anatomical, physiological and behavioural attributes. Third, although the focus of commercial ostrich production still remains in South Africa, the bird has become an important food and commercial animal that is now farmed in many parts of the world outside its native habitat, a development that has presented certain challenges for disease management and general husbandry (e.g. Tully and Shane, 1996). Finally, the exceptional body size of the ostrich and, hence, the large dimensions of its organs and organ systems provide an ideal model for morphological and physiological studies that are technically difficult or impossible to perform in smaller birds.

The conspicuous dearth of morphological and morphometric data on the ostrich lung can be attributed to various reasons: (i) the logistical difficulties of obtaining live healthy specimens from which fresh lung tissues can be adequately fixed for meaningful microscopy (in South Africa, in particular, although not strictly threatened, wild ostriches are protected and the extremely competitive and lucrative nature of commercial ostrich production presently constrains the availability of live specimens, especially for terminal experiments), (ii) problems with handling and restraining a large, highly irritable and dangerous bird and, (iii) inexplicable technical problems and uncertainties in fixing the lung

for microscopic studies. The ostrich lung is characteristic of the avian lung, being connected to capacious air sacs, some of which extend out of the coelomic cavity into the surrounding anatomical spaces and structures such as bones and even the skin (e.g. Bezuidenhout et al., 1999). Intratracheal instillation is technically the most direct method used for fixing lungs for microscopic morphometry and modelling: it preserves the vascular elements (particularly the erythrocytes) that are important elements in characterizing a lung's structural competence for gas exchange (e.g. Weibel, 1984; Bur et al., 1985). Furthermore, intravascular perfusion has been reported to cause a relatively greater degree of shrinkage than
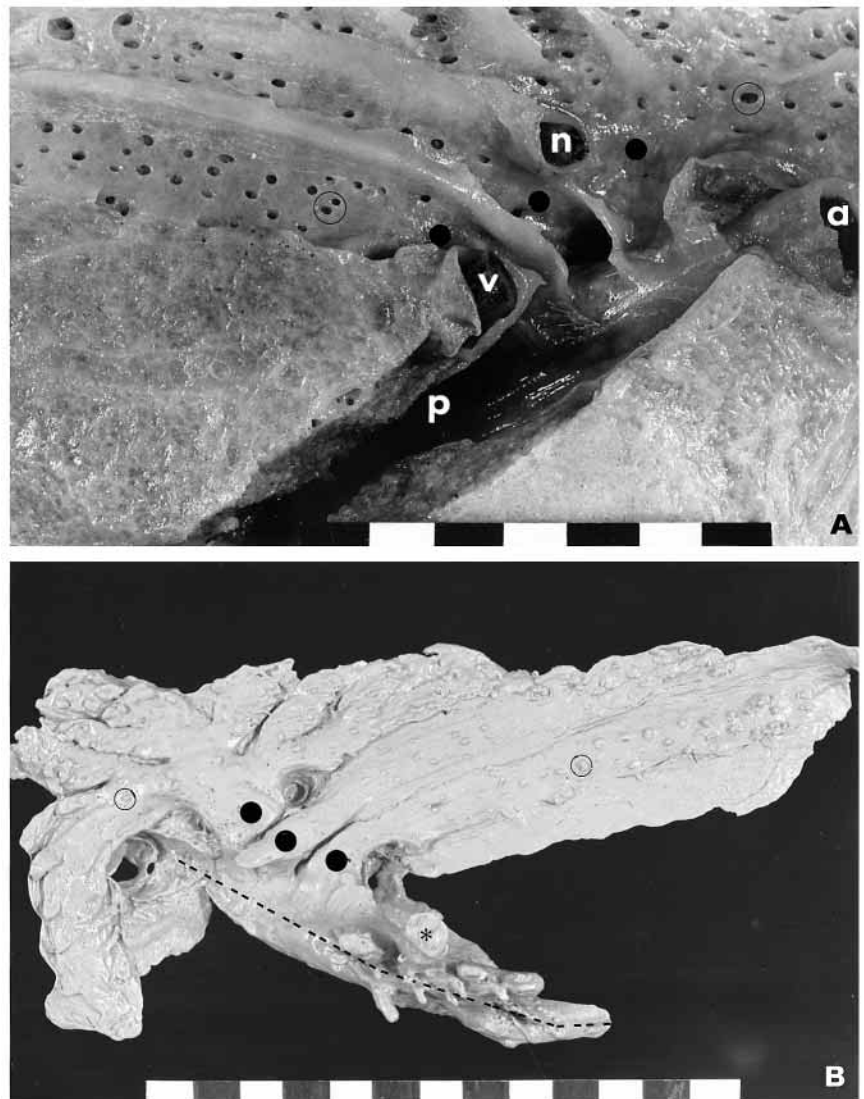


Fig. 3. (A) Close up of the hilus of the lung of the ostrich *Struthio camelus* showing three medioventral secondary bronchi (filled circles) arising from the primary bronchus (p) (dissected out). Parabronchi, circled; a, pulmonary artery; v, pulmonary vein; n, cranial branch of the pulmonary artery. Each gradation on the scale bar, 1 cm. (B) A dental plastic impression at the hilus and the intrapulmonary primary bronchus (dashed line) showing the three medioventral secondary bronchi (filled circles). Parabronchi, circled; asterisk, a mediodorsal secondary bronchus. Each gradation on the scale bar, 1 cm.

intratracheal instillation (e.g. Gil et al., 1979; Bachofen et al., 1982; Crapo et al., 1988). In birds in general and in the ostrich in particular, because of its exceptional size, fixing the lung by pouring the fixative down the trachea is like attempting to fill a large, highly perforated container with water. Since, according to physical laws, a fluid follows the line of least resistance, in such a design the fixative only reaches the lung if and when the air sacs and their extensive diverticulae (conceptually an external-limiting container) are filled up with fixative. At this point, the pressure build-up forces the fixative into the lung and subsequently into the very narrow terminal gas-exchange units, the air capillaries. Since the very nature of the lung is highly perforate, the fixation of the avian lung must be performed *in situ*, so even when the fixative stops flowing down the trachea (suggesting that the lung and the air sacs are filled up with fixative) there is no absolute certainty that the fixative has reached the most distant parts of the pulmonary airway system.

Our earlier attempts to fix the lungs of as many as six wild ostrich specimens in the field by intratracheal instillation with 2.3 % glutaraldehyde buffered with sodium cacodylate, a method that has been used with remarkable success on relatively smaller species of birds for microscopic morphometry (e.g. Dubach, 1981; Abdalla et al., 1982; Maina, 1982; Maina et al., 1989), was in all cases unsatisfactory. It would appear that, inexplicably, controlled laboratory conditions and the use of particular fixatives are important for the successful fixation of the ostrich lung. In the present study, we used CAS, a newly marketed fixative that offers particular advantage over conventional aldehyde-based fixatives in that it is not irritating to the eye and respiratory passages, causes minimal tissue shrinkage and maintains the tissue consistency almost in the *in vivo* state. Considering that only 31 of CAS was used to fix a large perforated lung and much of the fixative flowed down the trachea, IPPB and ostia into the capacious air sacs (a process confirmed after the coelomic cavity was opened), we envisage that the peroxide and alcohol vapours penetrated and fixed the lung tissue. Fixation of the mammalian lung using formalin vapour was first performed by Weibel and Vidone (Weibel and Vidone, 1962) and Weibel (Weibel, 1963), and subsequently by Dunnill (Dunnill, 1968). Using vapourized fixative on lungs is a judicious approach since it emulates the salient natural state that prevails during life, where the organ is filled with a gas (air), not a liquid. Owing to their much greater densities, liquid-based fixatives may cause changes in the size of the airways and location of the vascular elements of the lung. Unfortunately, many 'gaseous' fixatives, including vapourized formalin (e.g. Weibel, 1970/71), do not confer satisfactory preservation of tissues especially to the high level required for electron microscopy. Use of CAS, at least followed by 2.3 % glutaraldehyde buffered in sodium cacodylate, appears to offer satisfactory fixation for transmission electron microscopy (see Fig. 10).

The osmolarity of the fully constituted fixative is a critical factor in a morphometric analysis. A hyperosmotic fixative will cause tissue shrinkage, while a hypo-osmotic one may lead to tissue swelling and histological and ultrastructural
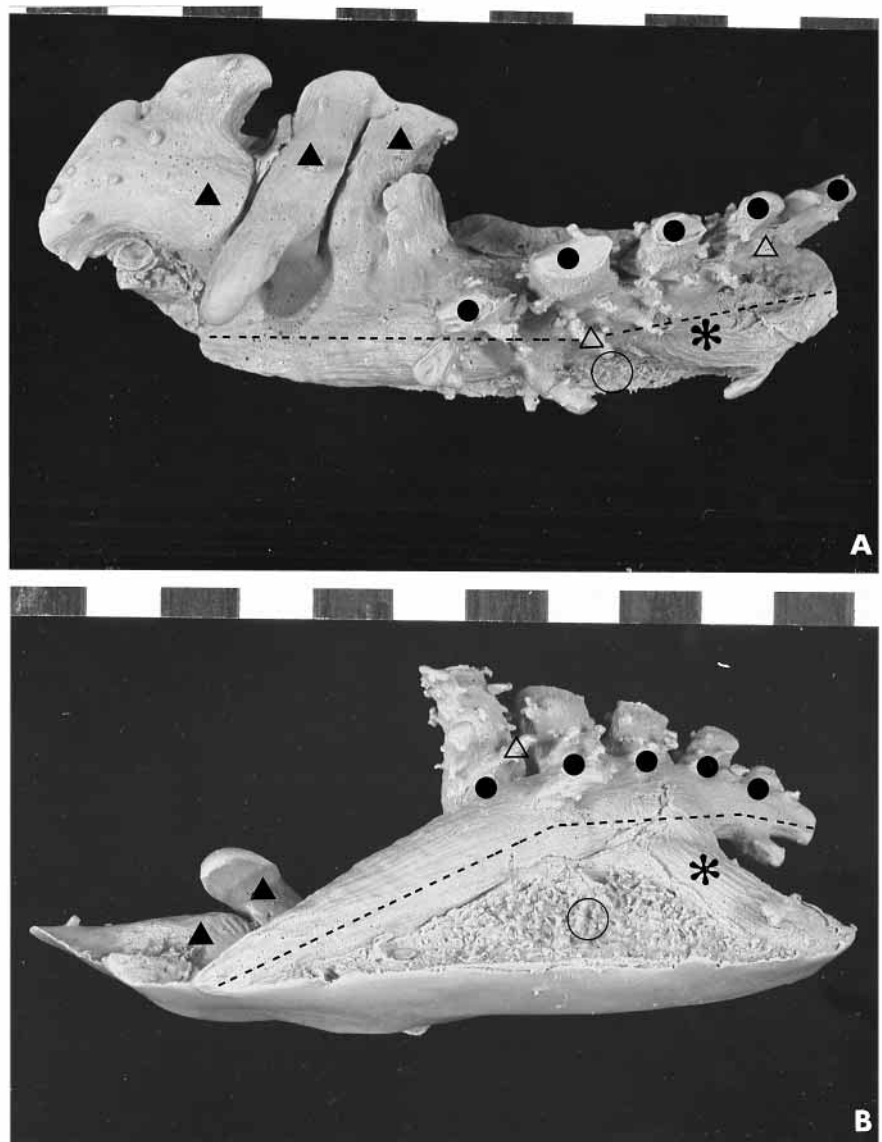


Fig. 4. (A,B) Views of dental plastic impressions of the hilus and the intrapulmonary primary bronchus (dashed line) of the lung of the ostrich *Struthio camelus* showing three medioventral secondary bronchi (filled triangles) and five mediodorsal secondary bronchi (filled circles). Open triangle, parabronchi; asterisk, lateroventral secondary bronchus; location of the neopulmonic parabronchi, circled. Each gradation on the scale bar, 1 cm.

imperfections. The degree of shrinkage caused by various fixatives and the contributions that buffers and fixatives themselves make to the overall osmolarity of a constituted fixative has long been debated (e.g. Weibel, 1963; Hayat, 1970; Eisenberg and Mobley, 1975; Barnard, 1976; Mathieu et al., 1978; Weibel, 1979; Lee et al., 1980; Mazzone et al., 1980; Wangensteen et al., 1981; Bastacky et al., 1985; Gehr and Crapo, 1988), and the issue is far from resolved. As a guiding principle, the fixative, buffer and other reagents used in processing biological tissues for microscopy should be chosen to maintain the qualitative and quantitative attributes of the tissues as close to their *in vivo* state as possible. Where necessary, shrinkage constants should be determined and, if significant, used to adjust the measurements. The osmolarity of CAS, the primary fixative used in the present, was $365\,\mathrm{mosmol\,l^{-1}}$ while that of the secondary fixative, i.e. 2.3 % glutaraldehyde buffered in sodium cacodylate, was $350\,\mathrm{mosmol\,l^{-1}}$. These values are reasonably close to the osmolarity of $340\,\mathrm{mosmol\,l^{-1}}$ determined for the blood plasma of the domestic fowl *Gallus gallus* var. *domesticus* (Sykes, 1971). Assuming that the osmolarity of the blood plasma in the ostrich is similar to that of the chicken, the use of approximately equiosmolar fixatives should have caused minimal shrinkage of the ostrich lung tissue.

The morphological features that were observed and the morphometric values that were determined in the ostrich lung suggest that this bird is particularly well adapted for gas exchange. The absence of the interparabronchial septa (IPS) indicates that the lung of the specimen examined in this study, which based on its body mass, would be considered to be juvenile, was fully developed. As can be inferred from earlier studies (e.g. Juillet, 1912; Locy and Larsell, 1916; Jones and Radnor, 1972), during the early stages of the development of the avian lung, the parabronchi (tertiary bronchi) are generally separated by septal connective tissue, giving them a somewhat hexagonal shape. In some species, the IPS persist throughout life, while in others, often the highly derived more energetic species (e.g. Duncker, 1972; Duncker, 1974; Duncker, 1979; Dubach, 1981; Maina et al., 1982), they are lost at various stages of development; when present, the IPS support the parabronchial blood vessels. Early maturity of the pulmonary system, as appears to occur in the ostrich, would be an adaptive feature in an energetic bird exposed to intense predation. The lung of the emu, the only extant

member of the family Dromaiidae and the most widespread of the Australian flightless birds (e.g. Cameron and Harrison, 1978), lacks IPS (Maina and King, 1989). Potentially, the rhea has a high aerobic capacity (Bundle et al., 1999), but no morphological investigation has been carried on its lung. In the ostrich, the very shallow atria that line the parabronchial lumina should minimize the diffusional distance of oxygen to the air capillaries, enhancing the gas-exchange efficiency. Unlike the species of birds that have so far been investigated (e.g. Maina, 1982; Maina, 1989; Maina et al., 1989), a
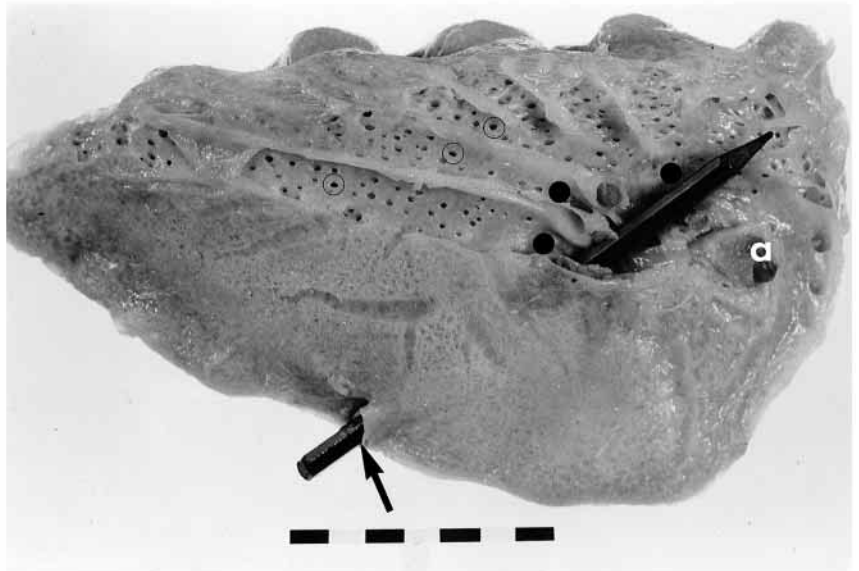


Fig. 5. Medial view of the left lung of the ostrich *Struthio camelus* showing the hilus and the three medioventral secondary bronchi (filled circles) arising from the primary bronchus (marked with a pencil). a, pulmonary artery; the arrow indicates ostium opening to the abdominal air sac. Each gradation on the scale bar, 1 cm. Open circles, parabronchi.



Fig. 6. Lateral view of the left lung of the ostrich *Struthio camelus* showing mediodorsal secondary bronchi (filled circles) arising from the primary bronchus. s, costal sulci; open circles, parabronchi. Each gradation on the scale bar, 1 cm.

conspicuous difference between the volumes of the right and the left lungs was observed in the ostrich: the volume of the left lung was 9 % greater than that of the right lung. Furthermore, conspicuous diameter, length and geometrical differences between the right and left EPPB were observed: the right EPPB was longer, narrower and more horizontal, while the left EPPB was shorter, wider and more vertical. The pulmonary and bronchial morphological differences that occurred in the ostrich were similar to those found in the human, but interestingly in the opposite pattern: in the human respiratory system, the right lung is larger than the left and the right primary bronchus is shorter, wider and more vertical (e.g. Romanes, 1972). Jones (Jones, 1982a) observed no significant difference in the lung mass between the left and the right lungs of the ostrich in the blood flow to the two lungs during resting and panting. Although Schulze (Schulze, 1908) described four groups of MVSB (his bronchi ventrales) in the ostrich, we could only find three MVSB, even after the preparation of plastic impressions that greatly improved the visualization of the dissected airways. It is difficult to establish the authenticity of Schulze's (Schulze, 1908) observations since his account completely lacks illustrations of pulmonary morphology. It was, however, quite evident in the present study that the number of MVSB in the ostrich lung could be mistaken, particularly because the large first MVSB bifurcates close to the primary bronchus (see Fig. 3, Fig. 5). The majority of birds have four MVSB (e.g. McLelland, 1989), some have five (e.g. cassowaries; Dotterweich, 1930) or even six (e.g. pelicans; e.g. Schulze, 1910). The developmental and functional significance of these differences is unclear.

Although wide-ranging extrapolations based on data from a single specimen may not be justifiable, among birds (e.g. Dubach, 1981; Maina et al., 1982; Maina, 1989; Maina et al., 1989), the ostrich lung has the highest volume density of the exchange tissue ($V_V$et) of 78.31 % (Table 2). Clearly, the high $V_V$et has formed at the expense of the lumina of the parabronchi, the secondary bronchi and the large blood vessels (Table 2). The large unventilated volume of the exchange tissue during protracted thermal panting may conceivably offer a substantial reservoir of carbon dioxide, presumably explaining the absence of respiratory alkalosis during such stressful conditions. Compared with the seven species of birds selected for comparison in Table 2, Table 3, Table 4 and Table 5 (for a comprehensive summary of the

pulmonary morphometric data available on the avian lung, see Maina, 1982; Maina, 1989; Maina et al., 1989), the mass-specific lung volume of the ostrich ($V_L M^{-1}$; 39.1 cm$^3$ kg$^{-1}$) was exceeded only by that of the hummingbird *Colibri coruscans* (Table 4). The τht of the ostrich lung was remarkably high (0.56 μm) (Table 5), comparable with that reported in the Humboldti penguin *Sphenicus humboldti* (0.53 μm) (Maina and King, 1987). The thick blood–gas (tissue) barrier in the penguin was attributed to a need to secure mechanical and functional integrity of the lung under high hydrodynamic pressure during dives (Welsch and Aschauer, 1986). While the ostrich is not subjected to same conditions, in a bird that may reach a height of 3 m, the lung may experience considerable
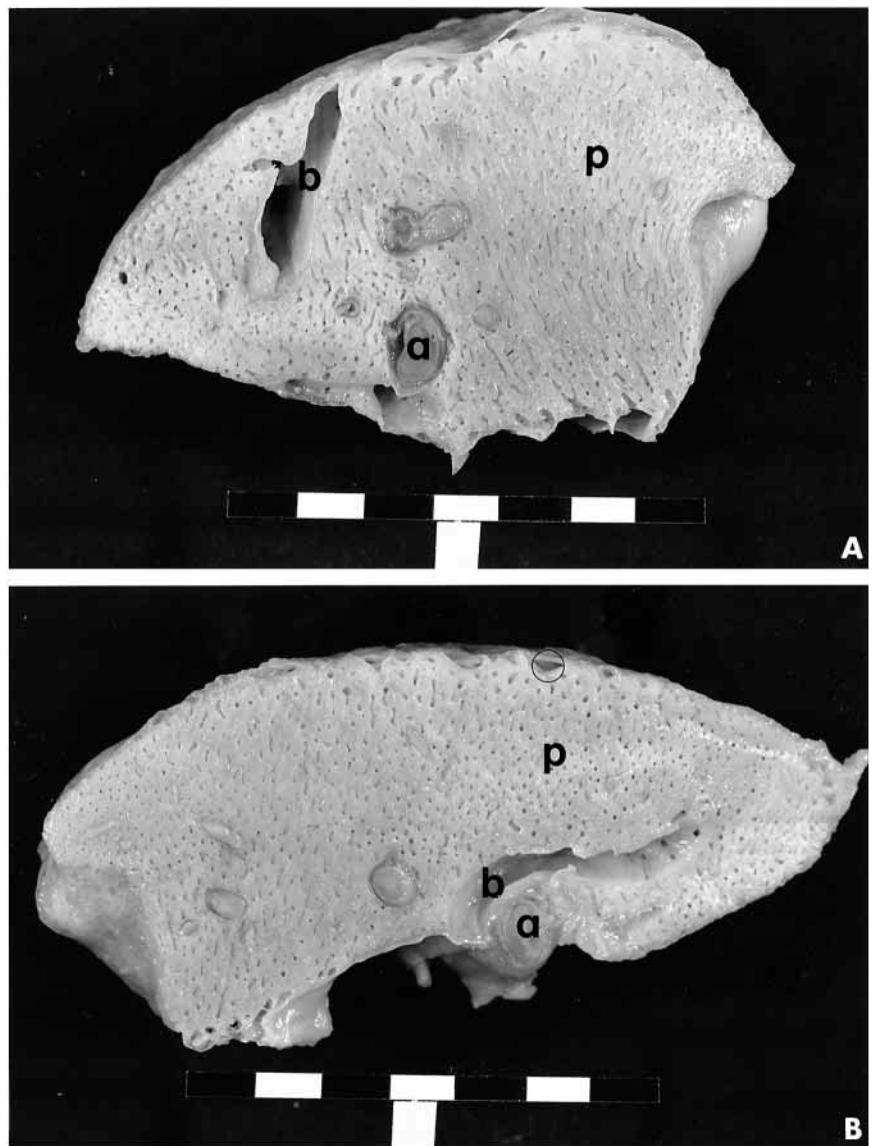


Fig. 7. (A) A slice of the lung of the ostrich *Struthio camelus* at the level of the third costal sulcus showing stacks of anastomosing parabronchi (p), a mediodorsal secondary bronchus (b) and a pulmonary artery (a). Each gradation on the scale bar, 1 cm. (B) A slice of the lung at the level of the first costal sulcus showing parabronchi (p), a medioventral secondary bronchus (b) and a pulmonary artery (a). The circle shows a secondary bronchus. Each gradation on the scale bar, 1 cm.

hypostatic congestion. This may necessitate the development of a thick tissue barrier to ensure physical fitness. Moreover, during high-speed running, when large volumes of blood pass through the lung, a thick tissue barrier may help to avoid damage to the pulmonary vasculature. Although measurements are lacking in the ostrich itself, systemic blood pressures in birds in general are remarkably high. Speckman and Ringer (Speckman and Ringer, 1963) determined a systolic blood pressure of 53 kPa in a resting domestic turkey *Melleagris gallopavo*. As commonly observed at *post mortem*, especially in domestic species of birds in which the functional capacities have been compromised through intense genetic breeding for properties, such as rapid weight gain and egg production (e.g. Smith, 1985; Gyles, 1989; Ross Breeders, 1999), sudden deaths in birds occasionally associated with fright result from arterial rupture (e.g. Carlson, 1960; Hamlin and Kondrich, 1969). Although the tissue barrier in the ostrich was remarkably thick compared with that of other birds (e.g. Maina, 1989; Maina et al., 1989), the plasma layer in the ostrich lung was remarkably thin (0.14 μm; Table 1). Compensatory adaptive structural strategies in the components of the air–haemoglobin pathway are a common feature of the design of the avian lung. In the penguin *Spheniscus humboldti*, e.g. while the tissue barrier was thick, $D_{LO_2}$ was greatly enhanced by a large $Vc$.

The mass-specific surface area of the tissue barrier ($St\,M^{-1}$) (Table 4) was relatively high in the ostrich (30.1 cm$^2$ g$^{-1}$) compared with that of non-flying birds such as the emu (5.4 cm$^2$ g$^{-1}$) (Maina and King, 1989), the penguin (18.1 cm$^2$ g$^{-1}$) (Maina and King, 1987) and the domestic fowl (8.7 cm$^2$ g$^{-1}$) (Abdalla et al., 1982). In the ostrich, an extensive respiratory surface area has offset a thick tissue barrier, giving a $Dt_{O_2}M^{-1}$ of 0.0022 ml O$_2$ s$^{-1}$ Pa$^{-1}$ kg$^{-1}$, the highest value in the two non-flying avian taxa (emu and penguin) selected for comparison (Table 5). The $Vc\,M^{-1}$ in the ostrich lung (6.25 cm$^3$ kg$^{-1}$) was only exceeded by that of the penguin *Spheniscus humboldti* (8.0 cm$^3$ kg$^{-1}$) (Table 5). Diving animals have high mass-specific blood volumes (e.g. Lenfant et al., 1970; Stephenson et al., 1988; Butler, 1991a), much of it being found in the lungs. The $Vc\,M^{-1}$ in the

ostrich was comparable with that of small volant birds such as the hummingbird *Colibri coruscans* (6.57 cm$^3$ kg$^{-1}$) and the house sparrow (6.4 cm$^3$ kg$^{-1}$). A large $Vc\,M^{-1}$ enhanced the $D_{LO_2}M^{-1}$ giving a mass-specific value of 0.00073 ml O$_2$ s$^{-1}$ Pa$^{-1}$ kg$^{-1}$ (Table 5): this value was only exceeded by that of the house sparrow (0.00093 ml O$_2$ s$^{-1}$ Pa$^{-1}$ kg$^{-1}$). Unfortunately, this variable was not determined by Dubach (Dubach, 1981) for the humming bird. The capillary loading, i.e. the ratio of the pulmonary capillary blood volume ($Vc$) to the respiratory surface area ($St$), indicates the degree of exposure of blood to air. In the ostrich, $Vc\,St^{-1}$ was 2.08 cm$^3$ m$^{-2}$, interestingly a value that was lower
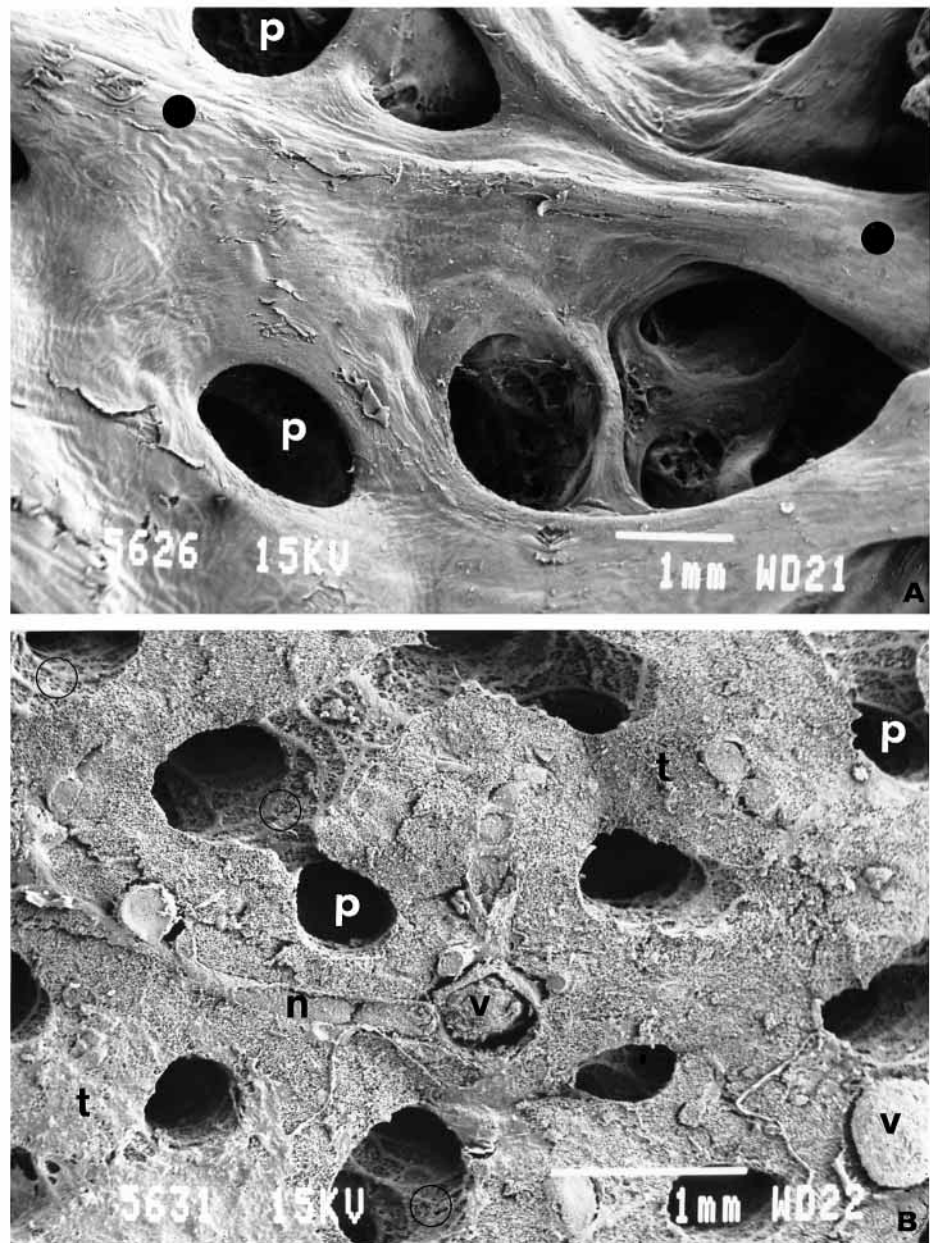


Fig. 8. (A) View of a medioventral secondary bronchus (filled circles) giving rise to parabronchi (p). (B) Parabronchial lumina (p) surrounded by exchange tissue (t); v, interparabronchial blood vessel. n, intraparabronchial blood vessel; Note the shallow atria (circled). Scale bars, 1 mm.

than that of the emu ($9.5\,cm^3\,m^{-2}$) and the penguin ($4.4\,cm^3\,m^{-2}$) (Table 5): the low $Vc\,St^{-1}$ in the ostrich is highly favourable for gas exchange since pulmonary capillary blood ($Vc$) is exposed to air over an extensive respiratory surface area. The substantial pulmonary morphometric differences between the ostrich and the emu may be explained by the fact that the latter lives in an environment that has relatively fewer predators.

Although the ostrich is flightless, it is an exceptionally energetic bird. It can achieve and sustain speeds as high as $90\;km\,h^{-1}$, making it the fastest ground-running bird (e.g. Cameron and Harrison, 1978; Fisher and Peterson, 1988). All the extant flightless birds have evolved secondarily from volant ancestors (e.g. Fisher and Peterson, 1988; Pough et al., 1989). Interestingly, they appear to have conserved the cardiopulmonary fitness of the latter (e.g. Brackenbury, 1991; Bundle et al., 1999). While considerable variation occurs among species, birds can increase their metabolic rates by factors ranging from 8 to 15 between rest and exercise (e.g. Lasiewski, 1963; LeFebvre, 1964; Tucker, 1968; Tucker, 1972; Torre-Bueno, 1985; Brackenbury and Avery, 1980; Grubb et al., 1983; Butler, 1991b). Birds trained to run on a treadmill can achieve maximum metabolic rates that approach those measured during flight (Brackenbury, 1991) and that far exceed those of terrestrial mammals under same conditions (e.g. Bundle et al., 1999). The relative metabolic capabilities of flying, running and swimming birds appear to be limited not directly by oxygen delivery but rather by the relative masses and aerobic capacities of the working muscles (e.g. Turner and Butler, 1988; Brackenbury, 1991). Bipedal runners such as the ratite birds use more energy for a given rate of force production because they require a greater mass of muscle to support their body weight (Roberts et al., 1998): on average, birds use 1.7 times more metabolic energy than the quadrupeds. In the rhea, the locomotory muscles constitute approximately 30 % of the body mass (Bundle et al., 1999). Energy constraints for locomotion may partly explain why the ostrich (the largest extant bird) is over 30 times smaller

than the elephant (the largest extant land mammal). The mass-specific resting rate of oxygen consumption ($\dot{V}_{O_2}\,M^{-1}$) of the ostrich is $4.72\,ml\,O_2\,min^{-1}\,kg^{-1}$ (Schmidt-Nielsen et al., 1969) compared with $3.91\,ml\,O_2\,min^{-1}\,kg^{-1}$ (Crawford and Lasiewski, 1968) or $4.2\,ml\,O_2\,min^{-1}\,kg^{-1}$ (Grubb et al., 1983) for the emu, and $5.28\,ml\,O_2\,min^{-1}\,kg^{-1}$ (Crawford and Lasiewski, 1968) for the rhea. The emu can increase its $\dot{V}_{O_2}$ approximately 11.4 times above resting (Grubb et al., 1983). Within 2 min of termination of an 11 km run at a speed of $17\;km\,h^{-1}$, the $\dot{V}_{O_2}\,M^{-1}$ of the ostrich was $31.35\,ml\,O_2\,min^{-1}\,kg^{-1}$ (Schmidt-Nielsen et al., 1969), giving
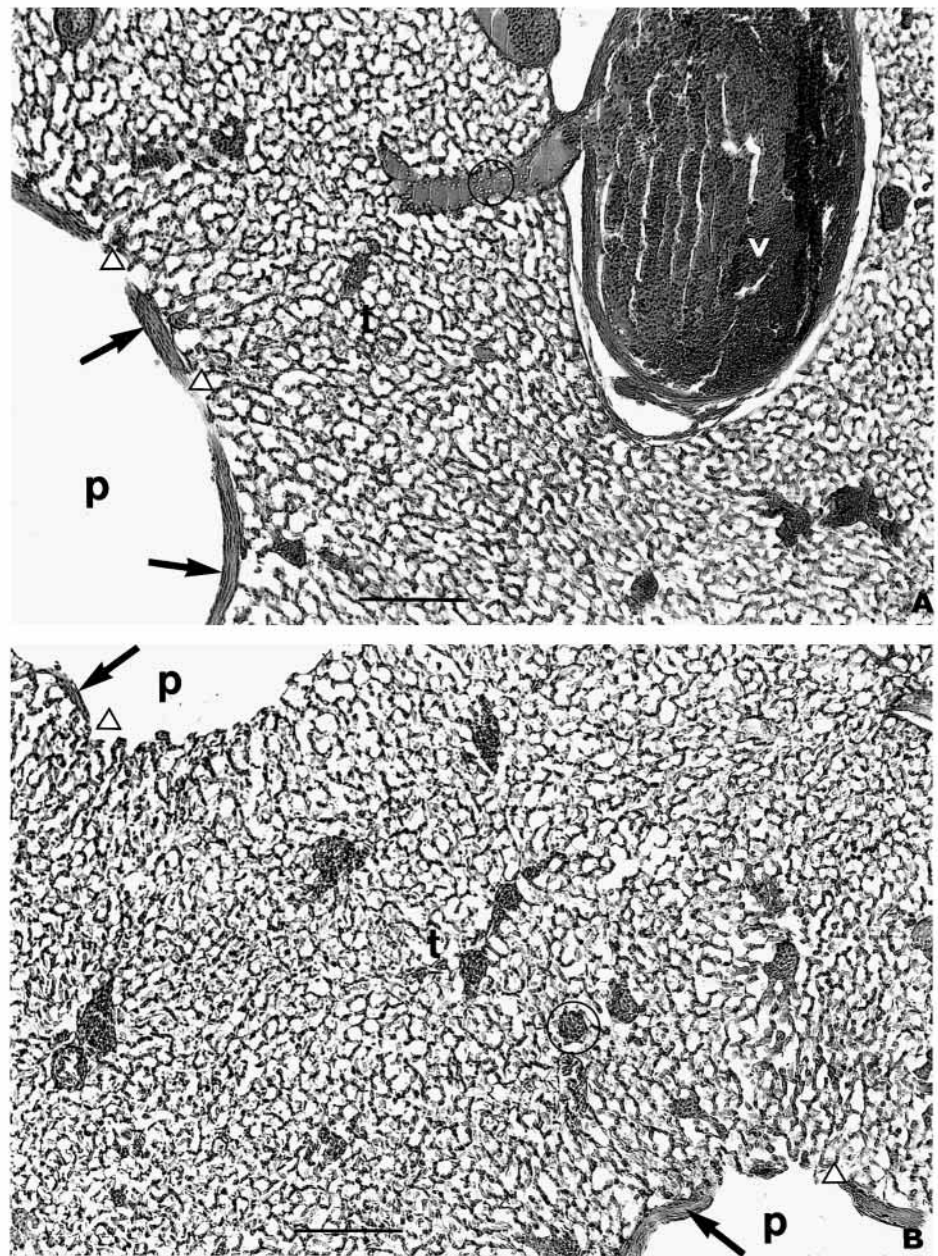


Fig. 9. (A,B) Views of the ostrich *Struthio camelus* lung showing an interparabronchial blood vessel (v). Intraparabronchial vessel, circled; t, exchange tissue; p, parabronchial lumen; arrows indicate atrial muscles. Note that interparabronchial septa are lacking in the lung and the atria (open triangle) are very shallow. Scale bars, $5\,\mu m$.
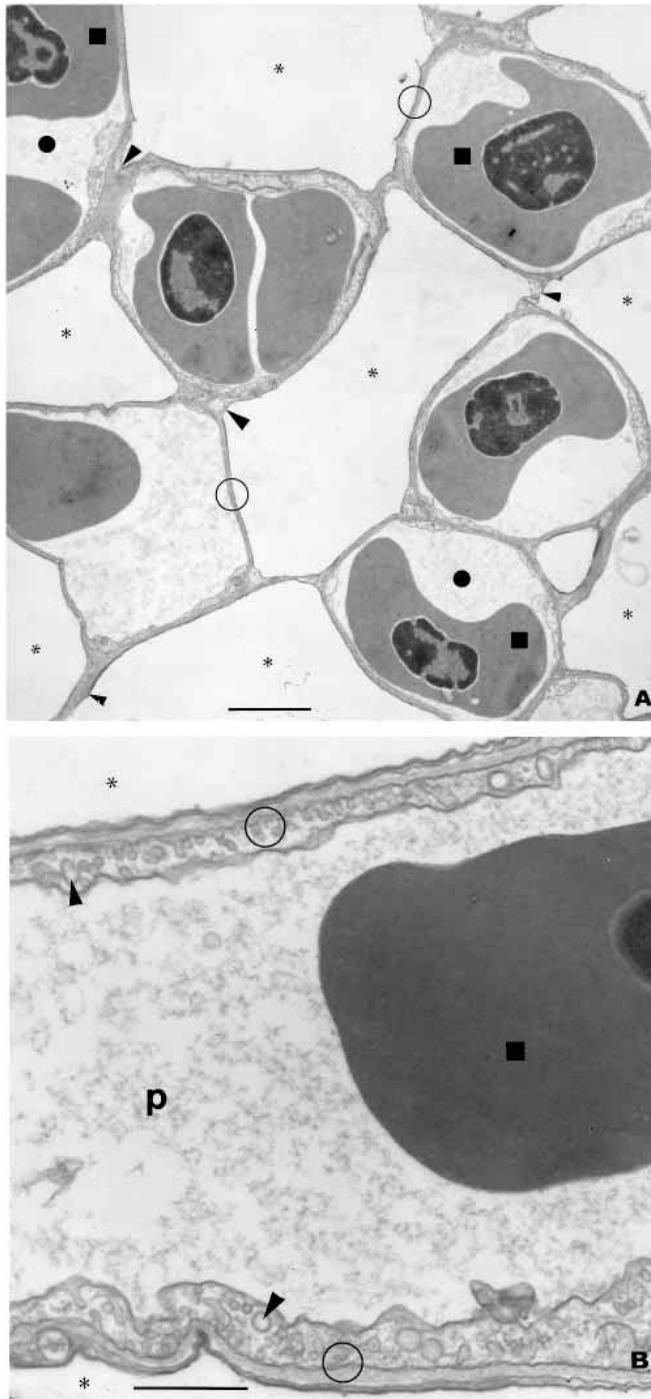
Fig. 10. (A) Exchange tissue of the lung of the ostrich *Struthio camelus* showing air capillaries (*) and blood capillaries (filled circles). The blood capillaries contain erythrocytes (filled squares). Open circles, blood–gas (tissue) barrier; filled arrowheads, tissue not involved in gas exchange, i.e. areas where blood capillaries join or where air capillaries lie adjacent to each other. Scale bar, 5 μm. (B) A blood capillary showing the blood–gas (tissue) barrier (open circle); blood plasma (p) and an erythrocyte (filled square). Note the sporadic attenuation of the blood–gas (tissue) barrier and the numerous micropinocytotic vesicles, filled arrowheads. Asterisks, air capillaries. Scale bar, 1 μm.

a factorial increase of $\dot{V}_{O_2}$ from rest to exercise of approximately 7. King and Farner (1961) pointed out that the $\dot{V}_{O_2}$ of the ostrich was approximately 30 % higher than that predictable from its body size. This was, however, disputed by Crawford and Schmidt-Nielsen (Crawford and Schmidt-Nielsen, 1967). In the rhea, Bundle et al. (Bundle et al., 1999) observed that, while running on an inclined treadmill, the upper limit of aerobic metabolism was 36 times the minimum resting rate, a factorial increase exceeding that reported for nearly all mammals: a $\dot{V}_{O_2max}$ of 171 ml $O_2$ min$^{-1}$ kg$^{-1}$ was reached at a speed of 14.4 km h$^{-1}$.

Since the ostrich and the emu can pant for a long time without undergoing respiratory alkalosis (Schmidt-Nielsen et al., 1969; Jones, 1982a; Jones, 1982b; Jones et al., 1983), an efficient expiratory aerodynamic valving (EAV) mechanism must operate in their respiratory systems. During resting breathing, the expired air is directed into the gas-exchange tissue of the paleopulmo through the openings of the MDSB. During thermal panting, the increased airflow from the caudal air sacs is directed into the IPPB onwards to the trachea. The hypoxaemic state that befalls a panting ostrich (Schmidt-Nielsen et al., 1969; Jones, 1982a; Jones, 1982b) or emu (Jones et al., 1983) may result from a combination of several factors, e.g. partitioning of pulmonary blood flow and/or shifts in the airflow pathways. Jones (Jones, 1982a) observed significant changes in the blood flow patterns between the paleopulmic and the neopulmonic regions of the ostrich lung when it changed from resting to panting. In other birds, however, the expired air is invariably directed into the MDSB (e.g. Brown et al., 1995) and then into the gas-exchange tissue regardless of the respiratory state. In the non-ratite birds, switching of the expiratory outflow pathways may be lacking or the process may be imperceptably less effective. The hyperventilatory airflow through the exchange tissue during thermal panting makes the nonratite birds hypocapnic and alkalotic (e.g. Bouverot et al., 1974; Marder et al., 1974; Marder and Arad, 1975; Ramirez and Bernstein, 1976; Krauzs et al., 1977). Compared with other birds, the ratite birds experience thermal stress under different conditions and circumstances: heat stress usually occurs when the birds are resting on the ground, a state in which the $\dot{V}_{O_2}$ is low. In the volant birds, however, the greatest need for heat dissipation occurs during exercise (flight), when $\dot{V}_{O_2}$ is high. While the ratites can afford to disengage the two processes (i.e. gas exchange and heat dissipation) this is impracticable in flying birds. Such functional conflicts suggest underlying morphological differences in the respiratory designs of the ratite and nonratite groups of birds. The ostrich has very well-developed capacious air sacs (Schmidt-Nielsen et al., 1969; Bezuidenhout et al., 1999): the volume of air sacs in a 100 kg ostrich is approximately 15 l, the caudal thoracic air sac being the largest (Schmidt-Nielsen et al., 1969). Boggs et al. (Boggs et al., 1998) suggested that locomotion in swimming birds might isochronally compress the caudal air sacs more than the cranial ones, forcing air through the lung: such a process may also enhance gas exchange in a running ostrich. Correlation
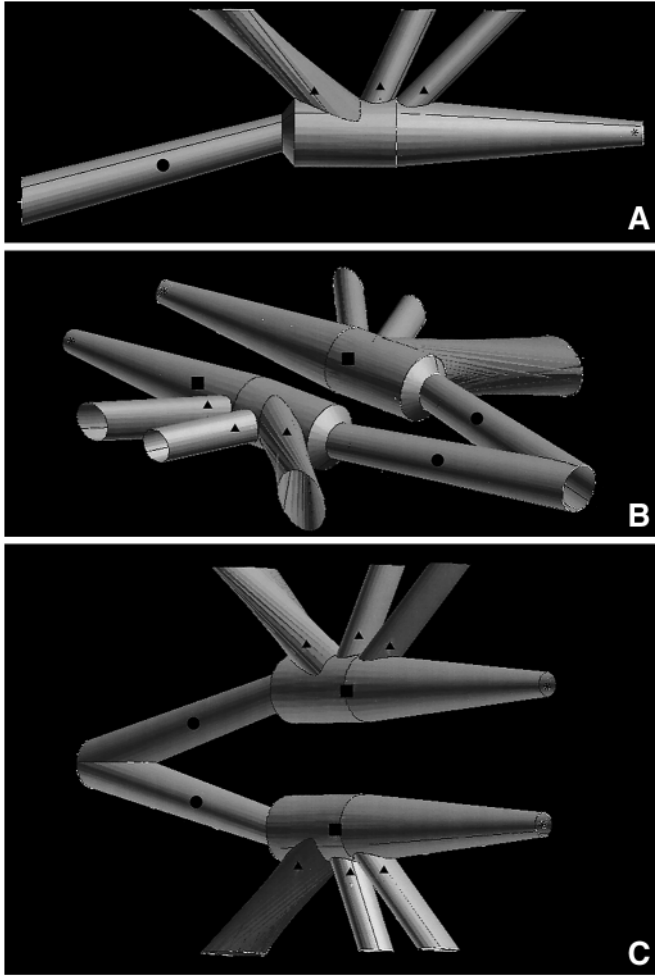
Fig. 11. Views of three-dimensional computer designs based on actual measurements of the bronchial system of the ostrich *Struthio camelus*. The air conduits that are shown include the extrapulmonary primary bronchi (EPPB, filled circles), the intrapulmonary primary bronchi (IPPB, filled squares) and the medioventral secondary bronchi (MVSB, filled triangles) (see also Fig. 2). The size and angulation of these air conduits are the most important features in the generation of inspiratory aerodynamic valving (IAV), i.e. the shunting of the inspired air past the openings of the MVSB. (A) Side view of an extrapulmonary primary bronchus, an intrapulmonary primary bronchus terminating in an ostium (asterisk) and three MVSB. (B,C) Views of the air-conduits in the right and left lungs. Note that only the sizes and the geometry at the origins of the MVSB, the most critical areas in IAV, are shown in the constructions. Subdivision and subsequent angulation of the bronchi is evident in Fig. 2 and in the actual specimens (Fig. 3, Fig. 4A, Fig. 5).

between locomotion and respiration has been reported in other groups of animals such as lizards (e.g. Carrier, 1991) and bats (e.g. Thomas, 1987). The ostrich can maintain its body temperature below 40 °C even when exposed to ambient temperatures of 56 °C for more than 6 h (Schmidt-Nielsen et al., 1969). Crawford and Schmidt-Nielsen (Crawford and Schmidt-Nielsen, 1967) suggested that, during thermal stress, the air sacs provide evaporative cooling as the gas-exchange

surfaces of the lungs are bypassed, while Bert (Bert, 1870) pointed out that the very survival of the ostrich in the Sahara was made possible by the role of the air sacs in cooling the body.

Morphological features of physiological significance were observed in the lung of the ostrich. The neopulmo is very poorly developed, consisting of a few laterodorsal secondary bronchi that arise from the most caudal part of the primary bronchus, their laterally directed parabronchi and the connections of the parabronchi with the caudal thoracic and abdominal air sacs. The MDSB are superficially located, making them easily accessible for sampling respiratory gases and experimental investigations of processes such as airflow dynamics. The ostrich lung conspicuously lacks a segmentum accelerans (SA), an epithelial tumescence at the terminal part of the EPPB (Maina and Africa, 2000). Wang et al. (Wang et al., 1992) associated the SA with inspiratory aerodynamic valving, i.e. the shunting of air past the openings of the MVSB. An SA was observed in the lung of the flightless domestic fowl (Maina and Africa, 2000) and may be of greater phylogenetic than functional significance. However, the domestic fowl has been domesticated from the wild jungle fowl *Gallus gallus* of South-East Asia for only the last 8000 years approximately (e.g. West and Zhou, 1988), which in evolutionary terms may not have been long enough for the loss of morphological features that may have been requisite for volancy. It is conceivable that, during thermal panting, the presence of an SA at the terminal part of the EPPB could impede the flow of the expired air from the IPPB to the trachea, deflecting some of it into the MVSB and subsequently into the cranial air sacs. Theoretically, this would create a nonrespiratory loop that would compromise both thermoregulation and gas exchange. The SA appears to be more important for shunting inspired air past the openings of the MVSB during resting (e.g. Banzett et al., 1987; Banzett et al., 1991; Wang et al., 1992). These investigators speculated that as a means of reducing the energetic cost of breathing, during exercise and other conditions that invoke hyperpnoea, the normally thick SA flattens almost to the diameter of the EPPB. Since the resting ostrich has a remarkably slow respiratory rate (six times per minute; e.g. Schmidt-Nielsen et al., 1969), it is interesting that an SA should be lacking in this bird. Jones (Jones, 1982a) suggested that the change in the airflow pattern from resting to panting in the ostrich could result from a scaling of the aerodynamic forces that govern flow in extremely large airways. The airflow dynamics in the remarkably large bronchial system of the ostrich may be totally different from those in the lungs of smaller birds.

In conclusion, for a flightless ratite bird, morphologically and morphometrically, the lung of the ostrich appears to present a singular design and exceptional structural refinements. These features conform to the high aerobic capacity attained and sustained by the bird and the thermal extremes that it survives through sustained panting on the ground, without incurring acid–base imbalance of the blood.

Table 3. *Volume densities (%) of the components of the exchange tissue of the lung of the ostrich compared with those of seven species of birds*

| | Air capillaries $V_{V}ac$ | Blood capillaries $V_{V}bc$ | Blood–gas (tissue) barrier $V_{V}bg$ | Tissue not involved in gas exchange $V_{V}te$ |
|---|---|---|---|---|
| Ostrich *Struthio camelus* | 61.19 | 20.41 | 12.69 | 5.71 |
| Emu *Dromiceius novaehollandiae* | 79.15 | 14.2 | 3.4 | 3.25 |
| Penguin *Spheniscus humboldti* | 34.36 | 51.04 | 14.6 | 14.6 |
| Domestic fowl *Gallus gallus* var. *domesticus* | 60.9 | 27.92 | 6.3 | 4.88 |
| Goose *Anser anser* | 62.03 | 32.43 | 4.24 | 1.3 |
| Hummingbird *Colibri coruscans* | 53.9 | 36.7 | 9.4 | – |
| Herring gull *Larus argentatus* | 53.68 | 35.92 | 7.04 | 3.36 |
| House sparrow *Passer domesticus* | 45.68 | 38.04 | 12.87 | 3.41 |

See Table 2 for sources of data.

Table 4. *Morphometric variables of the ostrich lung compared with those of seven species of birds*

| | $M$ (kg) | $V_{L}M^{-1}$ (cm$^3$ kg$^{-1}$) | $St\,M^{-1}$ (cm$^2$ g$^{-1}$) | $St\,Vet^{-1}$ (mm$^2$ mm$^{-3}$) |
|---|---|---|---|---|
| Ostrich *Struthio camelus* | 40 | 39.1 | 30.1 | 98.32 |
| Emu *Dromiceius novaehollandiae* | 30 | 36.7 | 5.4 | 83 |
| Penguin *Spheniscus humboldti* | 4.5 | 30.4 | 18.1 | 116 |
| Domestic fowl *Gallus gallus* var. *domesticus* | 2.141 | 12.6 | 8.7 | 172 |
| Goose *Anser anser* | 3.838 | 24.8 | 23.1 | 253 |
| Hummingbird *Colibri coruscans* | 0.007 | 42.9 | 87.1 | 389 |
| Herring gull *Larus argentatus* | 0.654 | 27.8 | 22.1 | 236.3 |
| House sparrow *Passer domesticus* | 0.025 | 29.8 | 63 | 388.9 |

See Table 2 for sources of data.
$M$, body mass; $V_{L}$, lung volume; $St$, surface area of the blood–gas (tissue) barrier; $Vet$, volume of the exchange tissue.

Table 5. *Morphometric variables of the ostrich lung compared with those of seven species of birds*

| English name | $Vc\,M^{-1}$ (cm$^3$ kg$^{-1}$) | $Vc\,St^{-1}$ (cm$^3$ m$^{-2}$) | $\tau ht$ (µm) | $Dt_{O_2}M^{-1}$ (ml O$_2$ s$^{-1}$ Pa$^{-1}$ kg$^{-1}$) | $D_{L_{O_2}}M^{-1}$ (ml O$_2$ s$^{-1}$ Pa$^{-1}$ kg$^{-1}$) |
|---|---|---|---|---|---|
| Ostrich *Struthio camelus* | 6.25 | 2.08 | 0.56 | 0.0022 | 0.00073 |
| Emu *Dromiceius novaehollandiae* | 0.93 | 9.5 | 0.232 | 0.00096 | 0.00014 |
| Penguin *Spheniscus humboldti* | 8 | 4.4 | 0.53 | 0.00141 | 0.00051 |
| Domestic fowl *Gallus gallus* var. *domesticus* | 1.63 | 1.62 | 0.318 | 0.00113 | 0.00013 |
| Goose *Anser anser* | 3.3 | 1.4 | 0.118 | 0.0085 | 0.00045 |
| Hummingbird *Colibri coruscans* | 6.57 | 0.95 | 0.099 | 0.0371 | – |
| Herring gull *Larus argentatus* | 3.3 | 1.46 | 0.153 | 0.00407 | 0.00037 |
| House sparrow *Passer domesticus* | 6.4 | 0.94 | 0.096 | 0.00074 | 0.00093 |

See Table 2 for sources of data.
$Vc$, volume of the pulmonary capillary blood; $M$, body mass; $St$, surface area of the blood–gas (tissue) barrier; $\tau ht$, harmonic mean thickness of the blood–gas (tissue) barrier; $Dt_{O_2}$, diffusing capacity of the blood–gas (tissue) barrier; $D_{L_{O_2}}$, total morphometric pulmonary diffusing capacity. The values given for $D_{L_{O_2}}$ are the means of the maximum and minimum values.

## List of symbols and abbreviations

| | |
|---|---|
| CFD | computational fluid dynamics |
| $De_{O_2}$ | diffusing capacity of the erythrocytes |
| $DL_{O_2}$ | total morphometric pulmonary diffusing capacity |
| $Dm_{O_2}$ | membrane diffusing capacity |
| $Dp_{O_2}$ | diffusing capacity of the plasma layer |
| $Dt_{O_2}$ | diffusing capacity of the blood–gas (tissue) barrier |
| EAV | expiratory aerodynamic valving |
| EPPB | extrapulmonary primary bronchi |
| IAV | inspiratory aerodynamic valving |
| IPPB | intrapulmonary primary bronchi |
| IPS | interparabronchial septa |
| LVSB | lateral ventral secondary bronchus |
| $M$ | body mass |
| MDSB | mediodorsal secondary bronchi |
| MVSB | medioventral secondary bronchi |
| SA | segmentum acccelerans |
| $St$ | surface area of the blood–gas (tissue) barrier |
| $S_V$ | surface density |
| $S_Vac$ | surface density of the air capillaries |
| $S_Vbg$ | surface density of the blood–gas barrier |
| $S_Vce$ | surface density of the capillary endothelium |
| $S_Ver$ | surface density of the erythrocytes |
| $S_Vte$ | surface density of the tissue not involved in gas exchange |
| $Vc$ | volume of the pulmonary capillary blood |
| $Vet$ | volume of the exchange tissue |
| $V_L$ | volume of the lung |
| $\dot{V}_{O_2}$ | rate of oxygen consumption |
| $V_V$ | volume density |
| $V_Vac$ | volume density of the air capillaries |
| $V_Vbc$ | volume density of the blood capillaries |
| $V_Vbg$ | volume density of the blood–gas (tissue) barrier |
| $V_Vet$ | volume density of the exchange tissue |
| $V_Vlb$ | volume density of the large (<0.5 mm diameter) blood vessels |
| $V_Vpb$ | volume density of the primary bronchus |
| $V_Vpl$ | volume density of the parabronchial lumen |
| $V_Vsp$ | volume density of the secondary bronchi and parabronchi |
| $V_Vsv$ | volume density of the small (20 μm>diameter>0.5) blood vessels |
| $V_Vte$ | volume density of the tissue not involved in gas exchange |
| $\tau hp$ | harmonic mean thickness of the plasma layer |
| $\tau ht$ | harmonic mean thickness of the blood–gas (tissue) barrier |
| $\tau t$ | arithmetic mean thickness of the blood–gas (tissue) barrier |

## References

**Abdalla, M. A., Maina, J. N., King, A. S., King, D. Z. and Henry, J.** (1982). Morphometrics of the avian lung. I. The domestic fowl (*Gallus gallus* variant *domesticus*). *Respir. Physiol.* **47**, 267–278.

**Bachofen, H., Ammann, A., Wangensteen, D. and Weibel, E. R.** (1982). Perfusion fixation for structure–function analysis: credits and limitations. *J. Appl. Physiol.* **53**, 528–533.

**Banzett, R. B., Butler, J. P., Nations, C. S., Barnas, J. L., Lehr, J. L. and Jones, J. H.** (1987). Inspiratory aerodynamic valving in goose lungs depends on gas density and velocity. *Respir. Physiol.* **70**, 287–300.

**Banzett, R. B., Nations, C. S., Wang, N., Fredberg, J. J. and Butler, J. P.** (1991). Pressure profiles show features essential to aerodynamic valving in geese. *Respir. Physiol.* **84**, 295–309.

**Barnard, T.** (1976). An empirical relationship for the formulation of glutaraldehyde based fixatives based on measurements of cell volume. *J. Ultrastruct. Res.* **54**, 478.

**Bastacky, J., Hayes, T. L. and Gelinas, R. P.** (1985). Quantitation of shrinkage during preparation for scanning electron microscopy: human lung. *Scanning* **7**, 134–140.

**Bert, P.** (1870). *Lecons sur la Physiologie Comprée de la Respiration.* Paris: Bailliére.

**Bezuidenhout, A. J.** (1981). The anatomy of the heart of the ostrich. DVSc thesis, University of Pretoria, South Africa.

**Bezuidenhout, A. J., Groenewald, H. B. and Soley, J. T.** (1999). An anatomical study of the respiratory air sacs in ostriches. *Ondersterpoort J. Vet. Res.* **66**, 317–325.

**Bligh, J. and Hartley, T. C.** (1965). The deep body temperature of an unrestrained ostrich, *Struthio camelus* recorded continuously by a radiotelemetric technique. *Ibis* **107**, 104–105.

**Boggs, D. F., Butler, P .J. and Wallace, S. E** (1998). Differential air pressures in diving tufted ducks, *Aythya fuligula*. *J. Exp. Biol.* **201**, 2665–2668.

**Bouverot, P., Hildwein, G. and LeGoff, D.** (1974). Evaporative water loss, respiratory pattern, gas exchange and acid–base balance during thermal panting in pekin ducks exposed to moderate heat. *Respir. Physiol.* **21**, 255–269.

**Brackenbury, J. H.** (1991). Ventilation, gas exchange and oxygen delivery in flying and flightless birds. In *Physiological Strategies for Gas Exchange and Metabolism* (ed. A. J. Woakes, M. K. Grieshaber and C. R. Bridges), pp. 125–147. Cambridge: Cambridge University Press.

**Brackenbury, J. H. and Avery, P.** (1980). Energy consumption and ventilatory mechanisms in exercising fowl. *Comp. Biochem. Physiol.* **66A**, 439–445.

**Brown, R. E., Kovacs, C. E., Butler, J. P., Wang, N., Lehr, J. and Banzett, R. B.** (1995). The avian lung: is there an aerodynamic expiratory valve? *J. Exp. Biol.* **198**, 349–2357.

**Bundle, M. W., Hoppeler, H., Vock, R., Tester, J. M. and Weyand, P. G.** (1999). High metabolic rates in running birds. *Nature* **397**, 31–32.

**Bur, S., Bachofen, H., Gehr, P. and Weibel, E. R.** (1985). Lung fixation by air way instillation: effects on capillary hematocrit. *Exp. Lung Res.* **9**, 56–66.

**Butler, J. P., Banzett, R. B. and Fredberg, J. J.** (1988). Inspiratory valving inavian bronchi: aerodynamic considerations. *Respir. Physiol.* **73**, 241–256.

**Butler, P. J.** (1991a). Respiratory adaptations to limited oxygen supply during diving in birds and mammals. In *Physiological Strategies for Gas Exchange and Metabolism* (ed. A. J. Woakes, M. K. Grieshaber and C. R. Bridges), pp. 235–257. Cambridge: Cambridge University Press.

**Butler, P. J.** (1991b). Exercise in birds. *J. Exp. Biol.* **160**, 233–262.

**Calder, W. A. and Dawson, T. J.** (1978). Resting metabolic rates of ratite birds: the kiwis and the emus. *Comp. Biochem. Physiol.* **60A**, 479–481.

**Calder, W. A. and Schmidt-Nielsen, K.** (1966). Evaporative cooling and respiratory alkalosis in the pigeon. *Proc. Natl. Acad. Sci. USA* **55**, 750–756.

**Calder, W. A. and Schmidt-Nielsen, K.** (1968). Panting and blood carbon dioxide in birds. *Am. J. Physiol.* **215**, 77–82.

**Cameron, A. D. and Harrison, C. J. O.** (1978). *Bird Families of the World*. Oxford: Elsevier-Phaidon.

**Carlson, C. W.** (1960). Aortic rupture. *Turkey Producer* January Issue, 18–26.

**Carrier, D. R.** (1991). Conflict in the hypaxial musculoskeletal system: documenting an evolutionary constraint. *Am. Zool.* **31**, 644–654.

**Crapo, J. D., Crapo, R. O., Jensen, R. L., Mercer, R. R. and Weibel, E. R.** (1988). Evaluation of lung diffusing capacity by physiological and morphometric techniques. *J. Appl. Physiol.* **64**, 2083–2091.

**Crawford, E. C. and Lasiewski, R. C.** (1968). Oxygen consumption and respiratory evaporation of the emu and the rhea. *Condor* **70**, 333–339.

**Crawford, E. C. and Schmidt-Nielsen, K.** (1967). Temperature regulation and evaporative cooling in the ostrich. *Am. J. Physiol.* **212**, 347–353.

**Dawson, W. R. and Schmidt-Nielsen, K.** (1964). Terrestrial animals in dry heat: desert birds. In *Handbook of Physiology*, section 4, *Adaptation to the Environment* (ed. D. B. Hill, E .F. Adolph and C. C. Wilber), pp. 481–492. Washington, DC: American Physiological Society.

**Dotterweich, H.** (1930). Versuch über den Weg der Atemluft in der Vogellunge. *Z.. Vergl. Physiol.* **11**, 271–284.

**Dubach, M.** (1981). Quantitative analysis of the respiratory system of the house sparrow, budgerigar and violet-eared hummingbird. *Respir. Physiol.* **46**, 43–60.

**Duncker, H.-R.** (1972). Structure of the avian lung. *Respir. Physiol.* **14**, 44–63.

**Duncker, H.-R.** (1974). Structure of the avian respiratory tract. *Respir. Physiol.* **22**, 1–34.

**Duncker, H.-R.** (1979). Die functionelle Anatomie des Lungen-Luftsack-Systems der vögel- mit besonderer Berücksichtigung der Greifvögel. *Prakt. Tierarzt.* **60**, 209- 218.

**Dunnill, M. S.** (1968). Quantitative methods in histology. In *Recent Advances in Clinical Pathology*, series V (ed. S. C. Dyke), pp. 401–416. London: Churchill.

**Eisenberg, B. R. and Mobley, B. A.** (1975). Size changes in single muscle fibers during fixation and embedding. *Tissue & Cell* **7**, 383–387.

**Else, P. L. and Hubert, A. J.** (1985). Mammals: an allometric study of metabolism at tissue and mitochondrial level. *Am. J. Physiol.* **248**, R415–R421.

**Fisher, J. and Peterson, R. T.** (1988). *World of Birds*. New York: Crescent Books.

**Gehr, P. and Crapo, J. D.** (1988). Morphometric analysis of the gas exchange region of the lung. In *Toxicology of the Lung* (ed. D. E. Gardner, J. D. Crapo and E. J. Massaro), pp. 1–42. New York: Raven Press.

**Gil, J., Bachofen, H., Gehr, P. and Weibel, E. R.** (1979). Alveolar volume-surface area relation in air- and saline-filled lungs fixed by vascular perfusion. *J. Appl. Physiol.* **47**, 990–1001.

**Grubb, B. R.** (1983). Allometric relations of cardiovascular function in birds. *Am. J. Physiol.* **14**, H567–H572.

**Grubb, B. R., Jorgensen, D. D. and Conner, M.** (1983). Cardiovascular changes in exercising emu. *J. Exp. Biol.* **104**, 193–201.

**Gruson, E. S.** (1976). *Checklist of Birds of the World*. London: William Collins.

**Gyles, N. R.** (1989). Poultry, people and progress. *Poultry Sci.* **68**, 1–8.

**Hamlin, R. L. and Kondrich, R. M.** (1969). Hypertension, regulation of heart rate and possible mechanism contributing to aortic rupture in turkeys. *Proc. Fedn. Am. Soc. Exp. Biol.* **28**, 451–456.

**Hayat, M. A.** (1970). *Principles and Techniques of Electron Microscopy: Biological Applications*, vol. 1. New York: van Nostrand Reinhold.

**Heusner, A. A.** (1982). Energy metabolism and body size. I. Is the 0.75 exponent of Kleiber's equation a statistical artifact? *Respir. Physiol.* **48**, 1–12.

**Heusner, A. A.** (1983). Mathematical expression of the effects of changes in body size on pulmonary function and structure. *Am. Rev. Respir. Dis.* **128**, S72–S74.

**Irving, L. and Krog, J.** (1954). Body temperatures of arctic and subarctic birds and mammals. *J. Appl. Physiol.* **6**, 667–680.

**Jeong, H., Tombor, B., Albert, R., Oltval, Z. N. and Barabási, A. L.** (2000). The large-scale organization of metabolic networks. *Nature* **407**, 651–654.

**Jones, A. W. and Radnor, C.** (1972). The development of the chick tertiary bronchus. II. The origin and the mode of production of the osmiophilic inclusion body. *J. Anat.* **113**, 303–324.

**Jones, J. H.** (1982a). Pulmonary blood flow distribution in panting ostriches. *J. Appl. Physiol.* **53**, 1411–1417.

**Jones, J. H.** (1982b). Hot ostriches: intraparabronchial blood flow changes during panting. *Fedn. Proc.* **41**, 1096.

**Jones, J. H., Grubb, B. and Schmidt-Nielsen, K.** (1983). Panting in the emu causes arterialhypoxemia. *Respir. Physiol.* **54**, 189–195.

**Juillet, A.** (1912). Recherches anatomiques, embryologiques, histologiques et comparatives sur le poumon des oiseaux. *Arch. Zool. Exp. Gén.* **9**, 207–371.

**King, J. R. and Farner, D. S.** (1961). Energy metabolism, thermoregulation and body temperature. In *Biology and Comparative Physiology of Birds*, vol. II (ed. A. J. Marshall), pp. 215–288. New York: Academic Press.

**King, J. R. and Farner, D. S.** (1964). Terrestrial animals in humid heat: birds. In *Handbook of Physiology*, section 4, *Adaptation to the Environment* (ed. D. B. Hill, E. F. Adolph and C. C. Wilber), pp. 603–624. Washington, DC: American Physiological Society.

**Kleiber, M.** (1947). Body size and metabolic rate. *Physiol. Rev.* **27**, 511–541.

**Kleiber, M.** (1961). *The Fire of Life: An Introduction to Animal Energetics*. New York: John Wiley & Sons.

**Krausz, S., Bernstein, R. and Marder, J.** (1977). The acid–base balance of the rock partridge (*Alectoris chukar*) exposed to high ambient temperatures. *Comp. Biochem. Physiol.* **57A**, 245–257.

**Lasiewski, R. C.** (1963). Oxygen consumption of torpid, resting, active and flying hummingbirds. *Physiol. Zool.* **36**, 122–140.

**Lasiewski, R. C. and Calder, W. A.** (1971). A preliminary allometric analysis of respiratory variables in resting birds. *Respir. Physiol.* **11**, 152–166.

**Lasiewski, R. C. and Dawson, W. R.** (1967). A re-examination of the relation between standard metabolic rate and body weight in birds. *Condor* **69**, 13–23.

**Lee, R. M. K. W., Garfield, R. E., Forrest, J. B. and Daniel, E. E.** (1980). Dimensional changes of cultured smooth muscle cells due to preparatory processes for transmission microscopy. *J. Microsc.* **120**, 85–91.

**LeFebvre, E. A.** (1964). The use of $D_2O^{18}$ for measuring energy metabolism in *Columba livia* at rest and in flight. *Auk* **81**, 403–416.

**Leighton, A. T., Siegel, P. B. and Siegel, H. S.** (1966). Body weight and surface area of chickens, *Gallus domesticus*. *Growth* **30**, 229–238.

**Lenfant, C., Johansen, K. and Torrance, J. D.** (1970). Gas transport and oxygen storage capacity in some pinnipeds and the sea otter. *Respir. Physiol.* **9**, 277–286.

**Locy, W. A. and Larsell, O.** (1916). The embryology of the birds lung. Based on observations of the domestic fowl. I. The external aspects of lung development. II. The development of the bronchial tree. *Am. J. Anat.* **19**, 447–504.

**Louw, G. N., Belonje, P. N. and Coetzee, H. J.** (1969). Renal function, respiration, heart rate and thermoregulation in the ostrich (*Struthio camelus*). *Scient. Pap. Namib Desert Res. Stn.* **42**, 43–54.

**Lutz, P. L., Longmuir, I. S. and Schmidt-Nielsen, K.** (1974). Oxygen affinity of bird blood. *Respir. Physiol.* **20**, 325–330.

**Macalister, A.** (1864). On the anatomy of the ostrich (*Struthio camelus*). *Proc. R. Irish Acad.* **IX**, 1–24.

**Maina, J. N.** (1982). Qualitative and quantitative observations of the lungs of aves with comments on the lung of chiroptera: a morphological study. PhD thesis, University of Liverpool, England.

**Maina, J. N.** (1984). Morphometrics of the avian lung. III. The structural design of the passerine lung. *Respir. Physiol.* **55**, 291–309.

**Maina, J. N.** (1987). Morphometrics of the avian lung. IV. The structural design of the charadriiform lung. *Respir. Physiol.* **68**, 99–119.

**Maina, J. N.** (1988). Scanning electron microscopic study of the spatial organization of the air- and blood-conducting components of the avian lung. *Anat. Rec.* **222**, 145- 153.

**Maina, J. N.** (1989). Morphometrics of the avian lung. In *Form and Function in Birds*, vol. 4 (ed. A. S. King and J. McLelland), pp. 307–368. London: Academic Press.

**Maina, J. N., Abdalla, M. A. and King, A. S.** (1982). Light microscopic morphometry of the lungs of 19 avian species. *Acta Anat.* **112**, 264–270.

**Maina, J. N. and Africa, M.** (2000). Inspiratory aerodynamic valving in the avian lung: morphological study of the extrapulmonary primary bronchus. *J. Exp. Biol.* **203**, 2865–2876.

**Maina, J. N. and King, A. S.** (1982). Morphometrics of the avian lung. II. The wild mallard (*Anas platyrhynchos*) and the greylag goose (*Anser anser*). *Respir. Physiol.* **50**, 299–313.

**Maina, J. N. and King, A. S.** (1987). A morphometric study of the lung of the Humboldti penguin (*Spheniscus humboldti*). *Zl. Vet. Med. C* **16**, C293–C297.

**Maina, J. N. and King, A. S.** (1989). The lung of the emu, *Dromiceius*

*novaehollandiae*: A microscopic and morphometric study. *J. Anat.* **163**, 67–74.

**Maina, J. N., King, A. S. and Settle, G.** (1989). An allometric study of the pulmonary morphometric parameters in birds, with mammalian comparison. *Phil. Trans. R. Soc. Lond. B* **326**, 1–57.

**Marder, J. and Arad, Z.** (1975). The acid–base balance of Abdim's stock (*Sphenorhynchus abdmii*) during thermal panting. *Comp. Biochem Physiol.* **51A**, 887–889.

**Marder, J., Arad, Z. and Gafni, M.** (1974). The effect of high ambient temperatures on acid–base balance of panting Bedouin fowl, *Gallus domesticus*. *Physiol. Zool.* **47**, 180–189.

**Mathieu, O., Claasen, H. and Weibel, E. R.** (1978). Differential effect of glutaraldehyde and buffer osmolarity on cell dimensions: a study of lung tissue. *J. Ultrastruct. Res.* **63**, 20–34.

**Mazzone, R. W., Kornblau, S. and Durand, C. M.** (1980). Shrinkage of lung after chemical fixation for analysis of pulmonary structure–function relations. *J. Appl. Physiol.* **48**, 382–385.

**McLelland, J.** (1989). Anatomy of the lungs and air sacs. In *Form and Function in Birds*, vol. 4 (ed. A. S. King and J. McLelland), pp. 221–279. London: Academic Press.

**McNab, B. K.** (1966). An analysis of the body temperatures of birds. *Condor* **68**, 47–55.

**Morony, J. J., Bock, W. J. and Farrand, J.** (1975). *Reference List of the Birds of the World*. New York: Department of Ornithology, American Museum of Natural History.

**Peters, R. H.** (1983). *The Ecological Implications of Body Size*. Cambridge: Cambridge University Press.

**Pough, F. H., Heiser, J. B. and McFarland, W. N.** (1989). *Vertebrate Life*. New York: Macmillan Publishing Co

**Ramirez, J. H. and Bernstein, M. H.** (1976). Compound ventilation during thermal panting in pigeons: a possible mechanism for minimizing hypocapnic alkalosis. *Fedn. Proc.* **35**, 2562–2565.

**Roberts, K. R., Weyand, P. G. and Taylor, C. R.** (1998). Energetics of bipedal running: metabolic cost of generating force. *J. Exp. Biol.* **201**, 2745–2751.

**Roché, M. G.** (1888). Prolongements intra-abdominaux des réservoirs cervicaux chez l'autruche. *Bull Soc. Philosmathique, Paris* **1**, 11–114.

**Romanes, G. J.** (1972). *Cunningham's Textbook of Anatomy*, 11th edition. London: Oxford University Press.

**Ross Breeders,** (1999). *Ross 308 Broiler Performance Objectives*. Newbridge: Ross Breeders.

**Schmidt-Nielsen, K.** (1964). *Desert Animals. Physiological Problems of Heat and Water.* Oxford: Clarendon.

**Schmidt-Nielsen, K.** (1984). *Scaling: Why is Animal Size so Important?* Cambridge: Cambridge University Press.

**Schmidt-Nielsen, K., Kanwisher, J., Lasiewski, R. C., Cohn, J. E. and Bretz, W. L.** (1969). Temperature regulation and respiration in the ostrich. *Condor* **71**, 341- 352.

**Schmidt-Nielsen, K. and Larimer, J. L.** (1958). Oxygen dissociation curves of mammalian blood and relation to body size. *Am. J. Physiol.* **195**, 424–428.

**Schulze, F. E.** (1908). Die Lungen des afrikanischen Strausses. *S.-B, Preuss. Akad. Wiss., Berlin* **1908**, 416–431.

**Schulze, F. E.** (1910). Über die Bronchi Saccales und den Mechanismus der Atmung bei den Vögeln. *S.-B, Preuss. Akad. Wiss., Berlin* **1910**, 537–538.

**Smith, J. H.** (1985). Breeders must respond to market trends. *Poultry-Misset Int.* **34** (January Issue), 51–58.

**Speckmann, E. W. and Ringer, R. K.** (1963). The cardiac output and carotid and tibial Blood pressure of the turkey. *Can. J. Biochem. Physiol.* **41**, 2337–2354.

**Stahl, W. R.** (1967). Scaling of respiratory variables in mammals. *J. Appl. Physiol.* **222**, 453–460.

**Stephenson, R., Turner, D. L. and Butler, P. J.** (1988). The relationship between diving activity and oxygen storage capacity in the tufted duck, *Aythya fuligula*. *J. Exp. Biol.* **141**, 265–275.

**Storer, R. W.** (1971a). Adaptive radiation in birds. In *Avian Biology*, vol. 1 (ed. D. S. Farner and J. R. King), pp. 147–188. New York: Academic Press.

**Storer, R. W.** (1971b). Classification of birds. In *Avian Biology*, vol. 1 (ed. D. S. Farner and J. R. King), pp. 1–17. New York: Academic Press.

**Suarez, R. K.** (1996). Upper limits of mass-specific metabolic rates. *Annu. Rev. Physiol.* **58**, 583–605.

**Suarez, R.K.** (1998). Oxygen and upper limits to animal design and performance. *J. Exp. Biol.* **201**, 1065–1072.

**Sykes, A. H.** (1971). Formation and composition of urine. In *Physiology and Biochemistry of the Domestic Fowl* (ed. D. J. Bell and B. M. Freeman), pp. 233–278. London: Academic Press.

**Thomas, S. P.** (1987). The physiology of bat flight. In *Recent Advances in the Study of Bats* (ed. M. B. Fenton, P. Racey and J. M. V. Rayner), pp. 75–99. Cambridge: Cambridge University Press.

**Torre-Bueno, J. R.** (1985). The energetics of avian flight at altitude. In *Bird Flight, BIONA Report 3* (ed. W. Nachtigall), pp. 45–87. Stuttgart: Gustav-Fischer.

**Tucker, V. A.** (1968). Respiratory physiology of house sparrows in relation to high altitude flight. *J. Exp. Biol.* **48**, 55–66.

**Tucker, V. A.** (1972). Respiration during flight in birds. *Respir. Physiol.* **14**, 75–82.

**Tully, T. N. and Shane, S. M.** (1996). Husbandry practices as related to infectious and parasitic diseases of farmed ratites. *Rev. Sci. Tech.* **15**, 73–89.

**Turner, D. L. and Butler, P. J.** (1988). The aerobic capacity of locomotory muscles in the tufted duck, *Aythya fuligula*. *J. Exp. Biol.* **135**, 445–460.

**Wang, N., Banzett, R. B., Nations, C. S. and Jenkins, F. A.** (1992). An aerodynamic valve in the avian primary bronchus. *J. Exp. Zool.* **262**, 441–445.

**Wangensteen, D., Bachofen, H. and Weibel, E. R.** (1981). Effects of glutaraldehyde or osmium tetroxide fixation of the osmotic properties of lung cells. *J. Microsc.* **124**, 189–196.

**Weibel, E. R.** (1963). *Morphometry of the Human Lung.* Berlin: Springer-Verlag.

**Weibel, E. R.** (1970/71). Morphometric estimation of pulmonary diffusion capacity. I. Model and method. *Respir. Physiol.* **11**, 54–75.

**Weibel, E. R.** (1979). *Stereological Methods*, vol. 1, *Practical Methods for Biological Morphometry*. London: Academic Press.

**Weibel, E. R.** (1984). *The Pathways for Oxygen: Structure and Function in the Mammalian Respiratory System*. Harvard, MA: Harvard University Press.

**Weibel, E. R.** (1990). Morphometry: Stereological theory and practical methods. In *Models of Lung Disease: Microscopy and Structural Methods* (ed. J. Gill), pp. 199–251. New York: Marcel Dekker.

**Weibel, E. R., Federspiel, W. J., Fryder-Doffey, F., Hisia, C. C. W., König, M., Stalder-Navarro, V. and Vock, R.** (1993). Morphometric model for pulmonary capacity. I. Membrane diffusing capacity. *Respir. Physiol.* **93**, 125–149.

**Weibel, E. R. and Knight, B. W.** (1964). A morphometric study on the thickness of the pulmonary air-blood barrier. *J. Cell Biol.* **21**, 367–384.

**Weibel, E. R. and Vidone, R. A.** (1962). Fixation of the lung by formalin steam in a controlled state of air inflation. *Am. Rev. Respir. Dis.* **84**, 856.

**Welsch, U. and Aschauer, B.** (1986). Ultrastructural observations on the lung of the emperor penguin (*Apternodytes forsteri*). *Cell Tissue Res.* **243**, 137–144.

**West, B. G., Brown, J. H. and Enquist, B. J.** (1999). The fourth dimension of life: fractal geometry and allometric scaling of organisms. *Science* **284**, 1677–1679.

**West, B. and Zhou, B. W.** (1988). Did chickens go North? New evidence for domestication. *J. Archeol. Sci.* **15**, 515–533.